Check for updates

International Journal of Climatology

International Journal of Climatology | RMetS

RESEARCH ARTICLE OPEN ACCESS

Statistical Downscaling of Daily Temperature and Precipitation From Regional Climate Models in Complex Mountain Terrain

Michael Matiu[1] | Anna Napoli[1,2] | Alberto Bellin[1] | Dino Zardi[1] | Bruno Majone[1]

[1]DICAM - Department of Civil, Environmental and Mechanical Engineering, University of Trento, Trento, Italy | [2]C3A - Center Agriculture Food Environment, San Michele all'Adige, Italy

Correspondence: Michael Matiu (michael.matiu@unitn.it)

Received: 10 March 2026 | **Revised:** 15 July 2026 | **Accepted:** 31 July 2026

Keywords: bias adjustment | EURO-CORDEX | Italian Alps | PCA | spatial downscaling

ABSTRACT

As greenhouse gas concentrations continue to rise and the world enters uncharted climate conditions, climate projections at the regional scale are becoming more and more crucial for planning adequate adaptation and mitigation strategies. In particular, in mountainous regions, high spatial resolution of climate information is crucial, as climate variables often exhibit strong variability over short spatial scales. Here, we (1) present a novel downscaling method based on principal components analysis (PCA), (2) evaluate the influence of separating bias adjustment from downscaling, (3) compare several methods for downscaling, including quantile delta mapping and a lapse rate adjustment and (4) assess the impact of multivariate bias adjustment using a snowfall climate index. We test all our objectives on an ensemble of 11 regional climate models driven by reanalysis for the period 1989–2008 in a cross-validation approach using two folds of 10 years. Our study area is Trentino-South Tyrol, a mountainous region in the Southeastern European Alps. Here, we exploit an existing high-resolution (1 km) gridded observational dataset for daily precipitation and temperature minima and maxima. Our results show that the novel PCA-based downscaling method performs well, especially for precipitation and accurately captures the observed spatial patterns. Separating bias adjustment from downscaling allows for combining different approaches; however, if quantile delta mapping is used for both bias adjustment and downscaling, then the separation increases errors. Among different downscaling methods, quantile delta mapping performs best overall; however, for temperature, simple lapse-rate adjustments also work reasonably well under average conditions. The multivariate bias adjustment shows minor benefits by accounting for inter-variable correlations, especially when the climate models did not reproduce observed correlations between temperature and precipitation. Overall, this research provides novel insights for the post-processing of climate model output in complex terrain, for example, when performing climate change impact models.

1 | Introduction

Mountain regions around the world are experiencing an accelerated warming compared to other areas, making them more vulnerable to climate change (Hock et al. 2019; Pepin et al. 2025). Due to elevation-dependent physical mechanisms, they respond more rapidly and more intensely to rising greenhouse gas concentrations than the global average and than other regions (Palazzi et al. 2019; Pepin et al. 2022). This enhanced warming significantly impacts mountain

Abbreviations: BA, bias adjustment; CDO, Climate Data Operators; DS, downscaling; GAM, generalised additive model; GCM, General Circulation Model; LR, (temperature) lapse rate; MBCn, Multivariate Bias Correction with N-dimensional PDF transform; PCA, principal components analysis; pr, precipitation; QDM, Quantile Delta Mapping; RCM, regional climate model; tasmax, maximum temperature; tasmin, minimum temperature.

This is an open access article under the terms of the Creative Commons Attribution License, which permits use, distribution and reproduction in any medium, provided the original work is properly cited.

© 2026 The Author(s). *International Journal of Climatology* published by John Wiley & Sons Ltd on behalf of Royal Meteorological Society.

ecosystems, including fauna and flora (Geppert et al. 2023; Rota et al. 2022; Verrall and Pickering 2020), human societies and economic activities (Adler et al. 2022). In mountain regions, where complex topography plays a crucial role, high spatial resolution is required to accurately capture key physical processes (Berthou et al. 2020). For the same reason, many impact studies require higher spatial resolutions than climate models can provide, for example, hydrological impact studies in mountain areas (Majone et al. 2016).

To achieve this goal, limited-area models, such as Regional Climate Models (RCMs), are driven by the output of General Circulation Models (GCMs) (Giorgi 2019). RCMs are then able to achieve a resolution better suited to represent most of the relevant atmospheric dynamics influenced by mountainous terrain than the GCMs (Kotlarski et al. 2015). For Europe, existing studies so far have relied mainly on results from the EURO-CORDEX initiative (the European branch of the Coordinated Regional Climate Downscaling Experiment of the World Climate Research Program), which coordinates a large number of climate modelling groups (Coppola et al. 2021).

However, even the current generation of model ensembles provided by EURO-CORDEX, with a horizontal resolution of 0.11°, is often considered too coarse for the terrain complexity characterising the European Alps. To overcome this limitation, further dynamical and statistical downscaling are often applied to GCM or RCM simulations. Dynamical downscaling involves further nesting of a higher-resolved model driven with boundary conditions from the RCM. For the Alps, ensembles of convection-permitting models have shown great improvements in the representation of extreme precipitation (Ban et al. 2021; Fosser et al. 2024; Pichelli et al. 2021), snow cover (Lüthi et al. 2019) and temperature by better resolving the physics and having finer spatial resolutions (Lucas-Picher et al. 2021). However, dynamical downscaling at convection-permitting scales is very computation and storage intensive, which is why simulations usually cover short time periods, fewer emission scenarios and the model ensemble is often smaller. On the other hand, statistical downscaling involves training a statistical model with coarse climate model output as predictors and local observations as predictands (target or reference). The relative benefits and limitations of both statistical and dynamical downscaling have been widely evaluated in the literature (e.g., Maraun et al. 2010; Fowler et al. 2007; Casanueva et al. 2016). Hence, today, both dynamical and statistical downscaling are considered complementary in many applications (Gutiérrez et al. 2019).

In the present study, we focus on statistical downscaling (DS) and bias adjustment (BA) approaches in a region with highly complex terrain within the European Alps, called Trentino-South Tyrol. Here, we leverage an existing high-resolution, observation-based spatial gridded dataset (Crespi et al. 2021). Statistical methods have shown great skill in reproducing many statistical properties, with quantile-based methods outperforming others such as weather generators, linear models and analogue-based methods (Gutiérrez et al. 2019). However, most statistical DS approaches focus on single locations (often meteorological stations) and only a few methods explicitly account for spatial dependency or spatial correlation between different locations (Widmann et al. 2019). In this study, we present a new method for downscaling climate model simulations based on principal components analysis (PCA). PCAs are widely used in climatology to extract important spatial features in gridded climate data (Wilks 2011). Our method was inspired by the asynchronous merging of spatial information employed by Frei et al. (2015) for creating sunshine grids in Switzerland, which was further refined for Austria by Hiebl et al. (2024).

Furthermore, it has been argued in the literature that BA and DS should be applied separately for quantile mapping (Volosciuk et al. 2017; Lange 2019). However, in practice, this is still rarely performed (Fischer et al. 2022) and the question arises as to what extent it offers practical advantage. Finally, multivariate BA methods that preserve inter-variable correlations should, in theory, perform better compared to univariate approaches. While some studies showed improvements with a multivariate approach (Cannon 2018; Zscheischler et al. 2019), others did not find a clear benefit in using multivariate BA (Meyer et al. 2019; Tootoonchi et al. 2022). Furthermore, it remains a challenge to extend the multivariate approach to consider not only inter-variable correlations but simultaneously account for spatial and temporal correlations (François et al. 2020). Moreover, depending on the bias adjustment approach, trade-offs need to be considered, since accounting for certain correlations, for example, inter-variable and spatial, might induce deficits in other correlations, for example, temporal (Allard et al. 2025).

In our study, we adopted downscaling and bias adjustment methods that could be applied in a climate change context using GCM-driven future scenarios and historical data that lack temporal synchrony with observations. We do not consider downscaling approaches that can only be applied to, for example, reanalysis. Our objectives with the present work are the following:

1. implement and evaluate a novel spatial downscaling technique based on PCA,
2. assess the impact of separating bias adjustment from downscaling using a quantile-based method,
3. evaluate multiple downscaling methods of varying complexity, including the spatial PCA-based method, in mountainous terrain,
4. identify the potential benefit of multivariate versus univariate bias adjustment with a simple multivariate snowfall index

The remainder of the paper is organised as follows: Section 2 introduces the study area and explains the methods. Section 3 presents the results and Section 4 discusses them. Finally, conclusions are given in Section 5.

2 | Data and Study Area

2.1 | Study Area

Downscaling methods were evaluated in Trentino-South Tyrol, which lies in north-eastern Italy on the southern European Alps (Figure 1). To the north, it borders the main Alpine chain and

10970088, 2026, 13, Downloaded from https://rmets.onlinelibrary.wiley.com/doi/10.1002/joc.70545 by CochraneItalia, Wiley Online Library on [03/11/2026]. See the Terms and Conditions (https://onlinelibrary.wiley.com/terms-and-conditions) on Wiley Online Library for rules of use; OA articles are governed by the applicable Creative Commons License

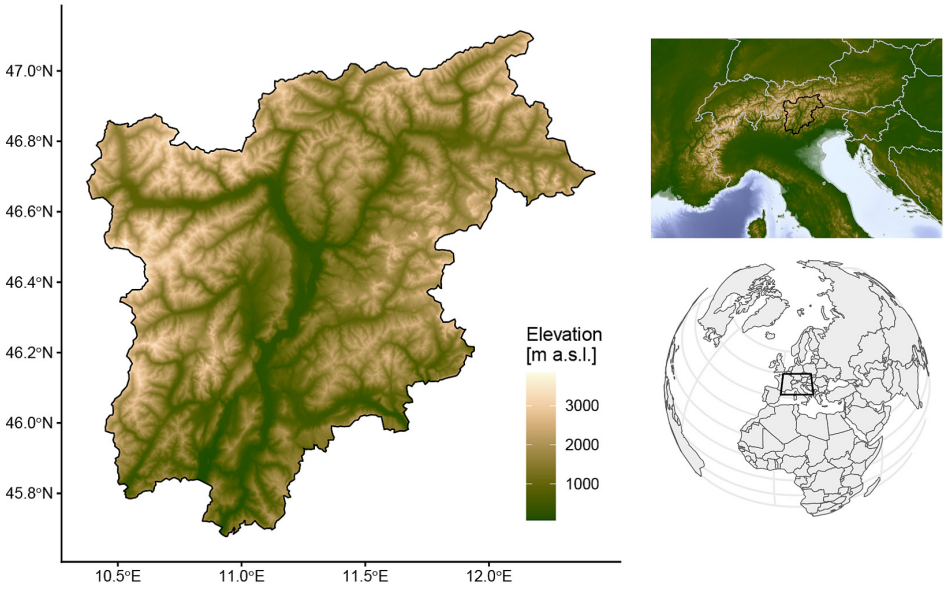


FIGURE 1 | Study area (Trentino-South Tyrol in north-eastern Italy) with elevation. The source of the elevation raster is the EU-DEM upscaled to 100 m for the study region (left) and the ETOPO Global Relief Model at 1 km for the context in the Alps (right).

to the south, the Po Valley, covering an area of approximately 13.600 km^2 and with elevations ranging from 200 to 3900 m.a.s.l. The region is characterised by a highly complex terrain with steep valleys and high mountain peaks. Based on a digital elevation model (EU-DEM v1.1) aggregated to 250 m resolution, the mean elevation of the region is around 1600 m with only 4% of flat areas, that is, with a slope below 5% (Crespi et al. 2021).

Its climate is influenced by the combination of various types of airflows: westerly moist advection from the Atlantic, easterly dry continental air masses and warm airflows from the Mediterranean area bringing humid winters and dry summers (Crespi et al. 2021). The geographic location within the Alps, along with the complex topography, induces high temporal variability and strong spatial gradients in climatic variables.

2.2 | Data

Observational data for the study regions were taken from Crespi et al. (2021). The dataset includes daily minimum temperature (tasmin), maximum temperature (tasmax) and daily precipitation (pr) at a 1 km spatial resolution for the period 1980–2020.

As a dataset to be downscaled and bias adjusted, we adopted the RCM simulations from the EURO-CORDEX initiative (Jacob et al. 2014) with boundary conditions from ERA-Interim. We adopted this modelling chain to avoid potential biases in the historical runs when GCMs are used as boundary conditions. Furthermore, this allows us to use evaluation metrics that require time synchrony, such as correlation and mean absolute error, whereas in GCM-driven simulations, only distribution-based metrics would have been possible. The common time period available to all reanalysis-driven RCMs was 1989 to 2008. We extracted the daily maximum (tasmax) and minimum temperature (tasmin) and precipitation (pr) from the EURO-CORDEX CMIP5-era on the EUR-11 grid (spatial resolution of 0.11°) available on ESGF (Earth System Grid Federation) servers as of 2024, which includes 11 RCMs (Table 1). To facilitate merging the RCM data with the observational dataset, we remapped the RCMs from the rotated-pole to a regular 0.11° grid using bilinear remapping with the Climate Data Operators (CDO).

TABLE 1 | List of Regional Climate Models (RCMs) used in the present study.

RCM model	Institute/group
ALADIN63	CNRM
CCLM4-8-17	CLMcom
COSMO-crCLIM-v1-1	CLMcom-ETH
HIRHAM5	DMI
HadREM3-GA7-05	MOHC
RACMO22E	KNMI
RCA4	SMHI
REMO2009	MPI-CSC
REMO2015	GERICS
RegCM4-6	ICTP
WRF381P	IPSL

Note: For further information on the models and modelling groups, we refer to Vautard et al. (2021) and references therein.

3 | Methods

In the following, we describe the overall evaluation framework and in detail the different bias adjustment and downscaling methods used in this study. Table 2 provides an overview of the methods with their main characteristics and how they are related to the study objectives. Method abbreviations follow a

10970088, 2026, 13, Downloaded from https://rmets.onlinelibrary.wiley.com/doi/10.1002/joc.70545 by CochraneItalia, Wiley Online Library on [03/11/2026]. See the Terms and Conditions (https://onlinelibrary.wiley.com/terms-and-conditions) on Wiley Online Library for rules of use; OA articles are governed by the applicable Creative Commons License

TABLE 2 | Labels of bias adjustment (BA) and downscaling (DS) methods, their combination, main characteristics and how they are related to study objectives.

Label	Obs. req. for BA	Obs. req. for DS	Variable	Spatial	Multivariate	Study objective
obs-ds-pcalm	()[a]	()[b]	TP	x		1
bads-qdm	x	x	TP			2, 3, 4
ba-qdm-ds-qdm	x	x	TP			2
ba-qdm-ds-qdm2	x	x	TP			2, 3, 4
ba-qdm-ds-pcalm	x	()[b]	TP	x		3, 4
ba-qdm-ds-lr	x		T			3
ba-qdm-ds-gam	x		T	x		3
bads-mbcn	x	x	TP		x	4
ba-mbcn-ds-qdm2	x	x	TP		x	4
ba-mbcn-ds-pcalm	x	()[b]	TP	x	x	4

Note: T in variable stands for temperature variables (minimum, maximum) and *P* for precipitation. More detailed descriptions and explanations of the labels can be found in the Section 3. Study objectives were to (1) test a novel spatial downscaling technique based on PCA, (2) test the impact of separating bias adjustment from downscaling, (3) evaluate multiple downscaling methods of varying complexity and (4) compare multivariate versus univariate bias adjustment.
[a]No BA step needed, since based on upscaled observations.
[b]Only used to derive the static PCs upfront, not used in the downscaling per se.

naming convention separated by dashes (–), identifying the methods used for bias adjustment (ba) and downscaling (ds).

The methods in a nutshell are *obs-ds-pcalm* (novel PCA-based downscaling evaluated on observations, not RCMs), *bads-qdm* (combined BA and DS with QDM), *ba-qdm-ds-qdm* (BA with QDM at the RCM scale, followed by a separate QDM for DS), *ba-qdm-ds-qdm2* (same as before, but different years used for DS, see Section 3.1 for details), *ba-qdm-ds-pcalm* (BA with QDM, DS with the PCA-based downscaling), *ba-qdm-ds-lr* (BA with QDM, DS with lapse-rates) and *ba-qdm-ds-gam* (BA with QDM, DS with generalised additive models). *bads-mbcn*, *ba-mbcn-ds-qdm2* and *ba-mbcn-ds-pcalm* are the multivariate extensions of *bads-qdm*, *ba-qdm-ds-qdm2* and *ba-qdm-ds-pcalm*.

3.1 | Evaluation Setup and Metrics

The overlapping time period between RCMs and observational data was 1989–2008. For validation, we conducted a twofold temporal split: first, the BA methods were trained on a 10-year subset extracted randomly and applied to the other 10-year subset. The procedure was then repeated by inverting the subsets. The random selection yielded the following years: 1990, 1992, 1993, 1994, 1995, 1997, 2000, 2003, 2004 and 2007 and correspondingly, the second set comprised the remaining years of the time span. Finally, both periods were combined before deriving the evaluation metrics. We used the following metrics: bias (sometimes called mean error), mean absolute error (MAE) and Pearson correlation coefficients.

After preliminary analyses, we found that the twofold temporal split led to high downscaling errors when the same years were used in both the BA and DS steps in *ba-qdm-ds-qdm*. Consequently, we further randomised the years in the DS step by taking five of them from each BA fold, such that the first DS fold contained the following years: 1991, 1993, 1994, 1995, 1996, 1999, 2000, 2001, 2003 and 2008. This was coined *ba-qdm-ds-qdm2*.

To assess the sensitivity of our results to the random splitting of the study period into two subsets, we repeated the procedure 20 times using different random partitions. The resulting variability was negligible and did not affect the overall conclusions. Figures S1 and S2 show that MAE and correlation remain stable across all the different replications for spring precipitation, both in terms of domain-averaged metrics and spatial patterns of errors. Only bias shows some variability between the replications, probably because there were only 10 years in each partition, which is rather low for estimating a robust climatology. Nonetheless, even the variability in bias between replications is much less than the difference between the methods. The other seasons and variables show similar results (not shown here).

We evaluated the downscaling methods separately in the temporal and spatial domains. For the temporal domain, the evaluation was performed at the seasonal level (December–January–February DJF, March–April–May MAM, June–July–August JJA, September–October–November SON). For individual grid cells, these were simply the seasonal metrics. For spatially aggregated metrics, we first computed the spatial averages before deriving the seasonal metric. In the spatial domain, the Pearson correlation was first computed at each time step for all grid cells in the downscaled and observational fields and then averaged seasonally.

Besides seasonal means, we also examined seasonal percentiles to assess the impact of the methods on extremes.

To assess the impact of multivariate bias adjustment, we chose a simple climatic index of snowfall that accounts for the dependence among precipitation, minimum and maximum temperatures.

10970088, 2026, 13, Downloaded from https://rmets.onlinelibrary.wiley.com/doi/10.1002/joc.70545 by CochraneItalia, Wiley Online Library on [03/11/2026]. See the Terms and Conditions (https://onlinelibrary.wiley.com/terms-and-conditions) on Wiley Online Library for rules of use; OA articles are governed by the applicable Creative Commons License

Other studies have used, for example, fire-weather indices (Allard et al. 2025); however, preliminary analyses indicated that the study area is too wet to show meaningful meteorological fire risk, so we did not adopt these indices. Snowfall was defined as the amount of precipitation times a fresh snow density of $\rho_{snow} = 100\ \mathrm{kg\ m^{-3}}$, only if the daily minimum temperature was below the threshold of $t_t = 2°C$. This was further linearly adjusted by the difference between maximum and minimum temperatures to account for days where the maximum temperature was above t_t, that is, part of the day was above the snowfall threshold:

$$N = \rho_{snow} \times \begin{cases} 0 & \text{if} \quad tasmin \geq t_t \\ pr & \text{if} \quad tasmax \leq t_t \\ pr \cdot \dfrac{t_t - tasmin}{tasmax - tasmin} & \text{otherwise} \end{cases}$$

Note that this is just a simple approximation of snowfall and does not claim to be exact, but rather sufficient to capture the multivariate dependency between temperature and precipitation, as shown in previous studies of snowfall in RCMs (e.g., de Vries et al. 2014; Frei et al. 2018). Nonetheless, the $t_t = 2°C$ threshold has been shown to identify snowfall days extremely well compared to snowfall observations (Zubler et al. 2014).

For the evaluation of precipitation and snowfall, observations were shifted back by 1 day to account for the fact that the observations correspond to the accumulated precipitation from 8 UTC of the previous day to 8 UTC of the current day, while the RCM values correspond to the accumulation in the current day (from midnight to midnight). Still, the remaining 8-h temporal shift is expected to deteriorate daily precipitation metrics.

3.2 | Spatial Downscaling Based on Principal Components Analysis

Here, we describe the methods we implemented to achieve the study objective (1), that is, the implementation and testing of a novel downscaling technique based on PCA. The method is inspired by the asynchronous merging of spatial information (Frei et al. 2015; Hiebl et al. 2024), where the authors extracted spatial information of sunshine duration from remote sensing observations using PCA and used this as an external drift component in the kriging interpolation of station observations of sunshine duration. The main advantage is that the two sources of information (remote sensing and stations) did not have to overlap temporally for the method to work. This is an important feature that is also required for downscaling methods in climate change applications, where calibration would be performed on GCM-driven historical runs.

In the present study, we adapt the method to a different context using spatial information from climate models and observations, which are both at different spatial resolutions. To the best of our knowledge, this is applied for the first time in such a context. In summary, the method uses PCA to extract time-invariant spatial fields that capture the major spatial gradients of the climate variables in the study area. With this method, the assumption is that these spatial features do not change over time but can vary by season. These time-invariant fields are then used for downscaling by estimating with a multiple linear regression the influence of each PC on the overall field for a given time step, that is, day.

Before applying any downscaling, PCA was applied seasonally (DJF, MAM, JJA, SON) to the daily observational grids of each variable (tasmin, tasmax, pr), yielding a total of 12 PCAs (4 seasons × 3 variables). As customary in PCA, the input matrix was centred, that is, the columns had their means subtracted. However, we did not scale the columns to unit variance, because only one variable (with the same unit) was included in each PCA. For precipitation, we removed days where the whole area showed zero precipitation in all grid-cells. Additionally, a square-root transformation was applied to precipitation, reducing the impact of extreme precipitation in the distribution tails and making the distribution closer to normal. The temperature data were not transformed. The number of retained PCs was based on the evaluation described below, along with results presented in Section 4.1. Note that the PCs are time-invariant fields, differing only by season.

To use the resulting PCA fields for downscaling, their spatial resolution must be matched to the coarse-scale RCM input. Hence, we upscaled the high-resolution PCs to the scale of the RCM and aligned their grids. The upscaling has been done by averaging the values within each coarser grid cell. Then, separately for each time step, we estimated with a multiple linear regression the influence of each coarse-scale PC on the daily RCM field of pr, tasmin or tasmax. For example, for precipitation:

$$pr_i^{RCM} = \beta_0 + \beta_1 \mathrm{PC1}_i^{\mathrm{upscaled}} + \beta_2 \mathrm{PC2}_i^{\mathrm{upscaled}} + \ \ldots\ + \epsilon, \tag{1}$$

where pr_i^{RCM} is the precipitation value at the i-th coarse RCM cell, β_k, $k = 0, 1, 2, \ldots$, are the coefficients of the linear model, $\mathrm{PC1}_i^{\mathrm{upscaled}}$ are the upscaled precipitation PCs to the coarse scale and ϵ are normally distributed errors with mean 0 and variance σ^2. The model (Equation 1) is fitted separately for each daily time step to the RCM data with the PCs of the respective season as independent variables. This regression estimates, for each day, the strength of each (time-invariant) PC field's influence on the current daily meteorological situation. For example, for precipitation, if the day shows a high north–south gradient in precipitation amounts, then the regression will result in a high β_1, since PC1 is related to north–south gradients (see Section 4.1 for more details on the PCA fields). On the other hand, if the day has only precipitation in the east, then β_1 of that day will be low, but β_2 will be high, since PC2 is related to east–west gradients. Consequently, each day will be characterised by a set of β_k coefficients that represent the meteorological situation of that particular day in terms of contributions of each PC, which themselves represent the major spatial features, to the overall field. The estimated coefficients $\hat{\beta}_k$ are then used to predict the downscaled field pr_j^{DS} at all the cells j of the high-resolution grid using the original high-resolution PCs (PC_j):

$$pr_j^{DS} = \hat{\beta}_0 + \hat{\beta}_1 \mathrm{PC1}_j + \hat{\beta}_2 \mathrm{PC2}_j + \ \ldots \tag{2}$$

Applying Equation (2) is where the actual downscaling occurs. The implicit assumption is that the coefficients that were

10970088, 2026, 13, Downloaded from https://rmets.onlinelibrary.wiley.com/doi/10.1002/joc.70545 by CochraneItalia, Wiley Online Library on [03/11/2026]. See the Terms and Conditions (https://onlinelibrary.wiley.com/terms-and-conditions) on Wiley Online Library for rules of use; OA articles are governed by the applicable Creative Commons License

estimated at the coarse scale also apply to the fine scale, which implies that there is spatial correspondence in the patterns between coarse and fine scale PCs. This approach also adjusts for different precipitation intensities at each respective day through the $\widehat{\beta}_k$ coefficients. Thus it is not required to adjust downscaled fields to match area-wide RCM precipitation.

Similar to the PCA, the linear model was trained on square-root transformed precipitation values and back-transformed after prediction. For temperature variables (tasmin, tasmax), the same model architecture as for precipitation was used, except that the PCs reflect other spatial features as for precipitation (e.g., PC1 is not a north–south gradient but elevation, see also Section 4.1) and no square-root transformation was applied.

We tested the impact of the number of PCs using a perfect-model setup. That is, we upscaled the observations to the coarse scale and used these to perform the downscaling. Then we compared the downscaled with the actual observations over the period 1989–2008. Hereafter, we call this method *obs-ds-pcalm*, implying that it is based on observations (obs), followed by the PCA-based downscaling (pcalm, because the PCA was used with a linear regression (lm) model).

Furthermore, we tested various alternative formulations. For temperature, we exchanged PC1 with elevation (similarly upscaled), since the first PC reflects ground elevation. For precipitation, we tested providing the precipitation as the product of intensity and occurrence, the latter being a binary variable indicating the presence or absence of precipitation. This was done using two separate regression models, rather than the model presented above. An ordinary linear model (Gaussian family) was used for the intensity. For occurrence, we fit a logistic regression (generalised linear model with the binomial family) using a threshold of 0.1 mm. For both models, the Equations (1) and (2) were the same. The variable occurrence is set to 1 if the predicted probability is greater than 0.5 and 0 otherwise. Two variants of this setup were investigated: (1) using the same input PCs as in the single-model setup; (2) applying a variant of the PCA called logisticPCA to derive PC fields of occurrence only (Landgraf and Lee 2020), using binary maps of precipitation occurrence as input to the PCA.

3.3 | Separating Bias Adjustment and Downscaling

Bias adjustment was performed using the trend-preserving Quantile Delta Mapping (QDM) method (Cannon et al. 2015) at the same spatial scale of the RCMs. Trend-preserving quantile methods were found to perform better than non-trend-preserving methods in a climate change context (Vrac et al. 2025). QDM is a bias adjustment method that removes systematic distributional errors while maintaining the climate model's projected trends. Unlike standard quantile mapping, which can artificially degrade trends, QDM preserves the modelled future change. For this, it extracts the climate model's change signal (relative change for precipitation, absolute change for temperature) relative to a historical period for all future quantiles. Then, it applies quantile mapping to correct distributional biases. Finally, it reintroduces the projected changes back into the bias adjusted output, thus ensuring that modelled trends in the distribution are retained. In the present case, the historical and projection period come from the twofold temporal split detailed in Section 3.1. For more details and formulae, we refer to Cannon et al. (2015).

We first upscaled the observational data, available at a finer grid than the RCMs, to match the RCM scale using conservative remapping in CDO. The observational dataset is confined to the political boundaries of the Trentino-South Tyrol region. Therefore, only the RCM cells with less than 5% of their area outside the boundary of the observational dataset were considered. We adopted this criterion because RCM grid cells covered only by a smaller fraction of the observational dataset might not be representative of the fraction of observations falling within the coarser RCM grid cell. QDM was applied month-by-month and gridcell-by-gridcell. Trend preservation was applied additively to temperature variables and multiplicatively to precipitation. For the wet-day threshold, we took the default value of 0.05 mm in the R-package MBC (Cannon 2023), which takes into account the drizzle effect in the RCMs.

The bias adjustment was followed by an additional application of QDM for downscaling. Quantile mapping methods have been widely used in the literature for downscaling in climate change assessments in Europe (e.g., Fischer et al. 2022), even though some authors argue that they should not be used for DS (Maraun 2016). Hereafter, we identify this sequence, bias adjustment with QDM, followed by downscaling with QDM, with *ba-qdm-ds-qdm*. We coined *ba-qdm-ds-qdm2* the application of bias adjustment with QDM, followed by downscaling with QDM but with different years in the DS step. *bads-qdm* was the application of bias adjustment and downscaling simultaneously in one step. Consequently, by comparing *bads-qdm*, *ba-qdm-ds-qdm* and *ba-qdm-ds-qdm2*, we can answer the study objective (2) of assessing the impact of separating the bias adjustment step from downscaling.

3.4 | Comparison of Different Bias Adjustment and Downscaling Methods

We named *ba-qdm-ds-pcalm* the application of PCA-based downscaling (Section 3.2) to RCM data, implying that first a bias adjustment has been performed on the coarse scale data, which was followed by the PCA-based downscaling.

For temperature, we tested two additional downscaling methods that do not require observational data as input. The first one uses lapse rate adjustments for the difference between the model elevation grid of the RCM and the high-resolution elevation. This method is labelled *ba-qdm-ds-lr*, again implying that a BA step was performed before the downscaling. Since it is not trivial to choose appropriate temperature lapse rates, we compared the existing literature (Rolland 2003; Liston and Elder 2006) and our observational input data, including, in addition to the grids, the station data used to create the gridded observational dataset of Crespi et al. (2021). All lapse rates agreed on the seasonal course with stronger gradients in summer than in winter; however, the different sources showed very different monthly

10970088, 2026, 13, Downloaded from https://rmets.onlinelibrary.wiley.com/doi/10.1002/joc.70545 by CochraneItalia, Wiley Online Library on [03/11/2026]. See the Terms and Conditions (https://onlinelibrary.wiley.com/terms-and-conditions) on Wiley Online Library for rules of use; OA articles are governed by the applicable Creative Commons License

lapse rates, especially for minimum temperatures (Figure S3). Liston and Elder (2006) did not distinguish between minimum and maximum temperature and showed stronger gradients than Rolland (2003), who analysed lapse rates in the Alps or as compared to our analysis based on the data of Crespi et al. (2021). Moreover, we found that the lapse rates calculated from the observational grid were consistently stronger than those calculated from the station input. We decided to trust most the local meteorological situation, so we chose lapse rates that were calculated based on the monthly climatology of the stations, which were used in the interpolation of the observational grid (Obs_StationClim in Figure S3). The final downscaled fields of minimum temperature are calculated using the following formula:

$$tasmin_j^{DS} = tasmin_i^{RCM} + LR_{month}^{tasmin} \cdot \left(elev_i^{RCM} - elev_j^{DS}\right), \tag{3}$$

where $tasmin_i^{RCM}$ is the minimum temperature of the RCM at gridcell i, $elev_i^{RCM}$ is the corresponding model elevation, $elev_j^{DS}$ is the elevation of the high-resolution gridcell j (target) and LR_{month}^{tasmin} is the lapse-rate of minimum temperature of the respective month in $K\ km^{-1}$. For maximum temperatures the same formula is applied equivalently with the respective monthly lapse-rates of maximum temperature.

The second additional method for downscaling temperature consisted of a 3-D (longitude, latitude, elevation) interpolation of the temperature fields from the RCMs using generalised additive models (GAMs) (Wood 2017). For each day, we trained a GAM to the RCM data: $tasmin_i \sim s_1(lon_i, lat_i) + s_2(elev_i)$, where s_1 is a two-dimensional thin-plate regression spline with maximum 25 degrees-of-freedom and s_2 is a one-dimensional thin-plate regression spline with maximum 5 degrees-of-freedom, lon_i, lat_i and $elev_i$ are the longitude, latitude and elevation of RCM cell i. This model was then applied to predict the DS field using the high-resolution coordinates lon_j and lat_j and elevation $elev_j$. This method is labelled *ba-qdm-ds-gam* and can be considered a spatially explicit downscaling method, besides the PCA-based one, implying that it is not applied cell-by-cell but considering the whole spatial field.

Finally, by comparing the different bias adjustment and downscaling methods (*bads-qdm*, *ba-qdm-ds-qdm2*, *ba-qdm-ds-pcalm*, *ba-qdm-ds-lr*, *ba-qdm-ds-gam*), we can answer the study objective (3) consisting in the evaluation of various downscaling models in complex terrain.

3.5 | Multivariate Bias Adjustment

Finally, to assess study objective (4), consisting in the evaluation of the benefits of multivariate bias adjustment, we used MBCn, the Multivariate Bias Correction with N-dimensional PDF transform (Cannon 2018). The multivariate correction was applied to all variables considered in the present work (tasmin, tasmax and pr). A few studies (e.g., Lange 2019) recommend not adjusting tasmin and tasmax together, but instead tasmin (or tasmax) and the diurnal temperature range (DTR, the difference between daily tasmax and tasmin), to avoid possible inconsistencies occurring when the adjusted tasmin is larger than the adjusted tasmax. We found this to be an extremely rare issue in our applications and therefore we decided to correct simultaneously tasmin and tasmax, also because such inconsistencies could arise in the univariate correction, too.

We applied the multivariate bias adjustment analogue to the univariate case described in Section 3.3, for both the separated BA and DS, as well as the joint BA and DS. The respective labels are *bads-mbcn*, *ba-mbcn-ds-qdm2* and *ba-mbcn-ds-pcalm*. We did not apply it to *ba-mbcn-ds-qdm* and the two downscaling methods that only work for temperature (*ba-qdm-ds-lr* and *ba-qdm-ds-gam*).

4 | Results

In the following, we present results (text, figures and tables) by alternating between the different seasons in order to improve clarity. The results for the seasons not mentioned in the ensuing text can be found in the appendix.

4.1 | Evaluation of PCA-Based Downscaling

The PCA analysis of the observational grids revealed the major spatial features of the study region. For precipitation, the first PC explained between 32% (for summer) and 48% (for winter) of the variability and was related to the north–south gradient (Figure 2 for winter and Figure S6 for the other seasons). The second PC explained 12%–14% of variability and was related to east–west gradients. The explained variance for each PC, as well as the cumulative one, can be found in the Supporting Information (Figures S4 and S5). For temperature, the first PC reflects elevation and explains 91%–97% (depending on season) of variability (Figure 2 for tasmin in winter; Figure S7 for the other seasons and Figure S8 for tasmax). The remaining PCs explain only minor amounts of variability and reflect spatial gradients or other factors related to elevation (i.e., inversion in winter).

The evaluation of the PCA-based downscaling in the perfect model setup (i.e., applied to upscaled observations) enabled us to identify the best variant and the number of PCs to keep for downscaling. For precipitation, downscaling bias decreased strongly after including the fourth PC, especially in terms of the variability across the gridcells (shown in the violin plots in Figure 3a). However, biases gradually decreased further the more PCs were included. This is true for summer (Figure 3a) and also for the other seasons (Figure S9). We found that using a single model for precipitation produced very similar metrics compared to combining two separate components for occurrence and intensity, but the single model performed slightly better with lower median bias (Figure 3a). Exchanging the PCA fields used for occurrence in the two-step model with fields from a logistic PCA deteriorated metrics with increasing bias and increasing MAE (Figure 3a).

On the other hand, the distribution of errors for temperature widened if more PCs were used. For example, for summer minimum temperatures, using more than 6 PCs resulted in a higher frequency of negative bias and higher MAE (Figure 3b), while for the other seasons or for maximum temperature, this already happened after 4 PCs (Figures S10 and S11). In fact, we observed very little change in metrics when using more than 3 PCs for

10970088, 2026, 13, Downloaded from https://rmets.onlinelibrary.wiley.com/doi/10.1002/joc.70545 by CochraneItalia, Wiley Online Library on [03/11/2026]. See the Terms and Conditions (https://onlinelibrary.wiley.com/terms-and-conditions) on Wiley Online Library for rules of use; OA articles are governed by the applicable Creative Commons License

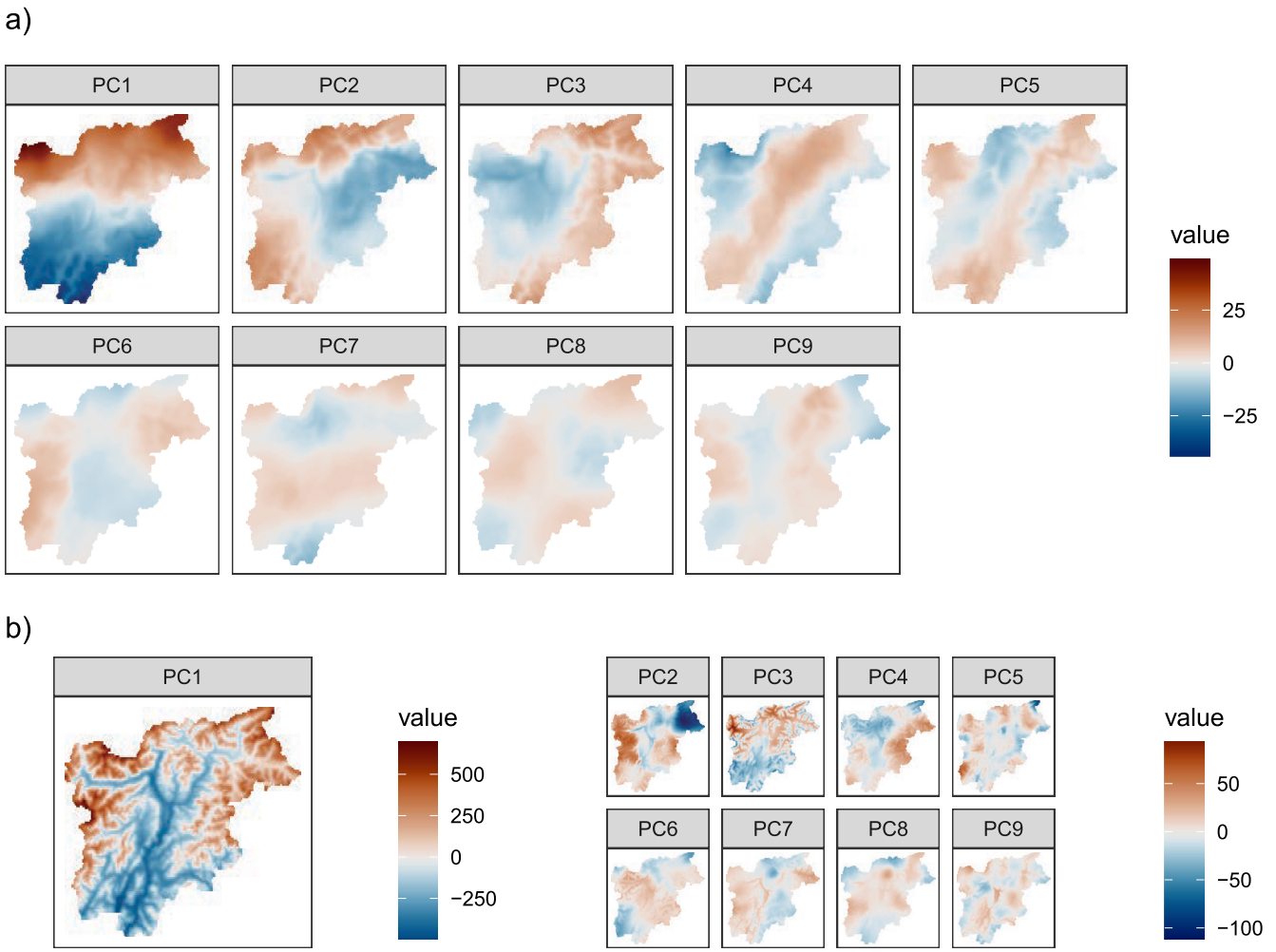


FIGURE 2 | Principal Components Analysis of the observational grids. The first 9 PCs are shown for precipitation (a) and daily minimum temperature (b) for winter (DJF, December–February).

temperature. Moreover, using elevation instead of PC1 did not improve downscaling results either. While the median bias was the same when using elevation or PC1 as the first PC, with elevation the distribution included higher biases and higher MAE (Figure 3b).

Based on these results, we chose to use 9 PCs for precipitation with the single component model because, even though the metrics significantly improved after having 4 PCs, metrics were slightly better with 9 PCs. For temperature variables, we chose 3 PCs with PC1 as first PC for the downscaling of RCMs.

4.2 | Separating Bias Adjustment and Downscaling With a Quantile Mapping Technique

At the coarse scale, bias adjustment effectively removed average bias from the RCMs (Figure S12). For temperature, BA also dealt with the impact of topographic smoothing in RCMs, which is the smoothing of surface elevation in climate models for numerical reasons (Figure S12). Domain-averaged biases were negligible after the adjustment (Figure S13). For tasmin, raw model output showed domain-averaged biases between −6.2°C and 3.7°C, while after BA, biases were reduced to $(-0.2, -0.1)$°C. For precipitation, biases were reduced from the range of $(-15\%, 120\%)$ to $(-2\%, 13\%)$. While quantile mapping techniques, by design, should reproduce the distribution of observations exactly, the remaining biases are likely caused by the applied two-fold cross-validation approach.

We obtained similar results by following the bias adjustment with another application of QDM for downscaling (*ba-qdm-ds-qdm*, *ba-qdm-ds-qdm2*) or performing a combined bias adjustment and downscaling (*bads-qdm*), with the combined approach showing a slightly better downscaling performance (Figure 4). Winter minimum temperatures showed negligible spatially-averaged biases (<0.01°C) for all three methods (Figure 4a); however, correlations were higher and MAE was lower for *bads-qdm* and *ba-qdm-ds-qdm2* than for *ba-qdm-ds-qdm* (Figure 4a). Spatially-averaged winter precipitation biases were much higher than for temperature (Figure 4b). The median over all 11 RCMs was 8% (range: 2, 13) for *bads-qdm*, 9% (6, 18) for *ba-qdm-ds-qdm2* and 28% (12, 50) for *ba-qdm-ds-qdm*. Similarly, correlations and MAE were best for *bads-qdm*, followed by *ba-qdm-ds-qdm2* and *ba-qdm-ds-qdm* (Figure 4b).

Results are similar in the other seasons, as well as for maximum temperature (Figures S14, S15 and S16). Consequently, there

10970088, 2026, 13, Downloaded from https://rmets.onlinelibrary.wiley.com/doi/10.1002/joc.70545 by CochraneItalia, Wiley Online Library on [03/11/2026]. See the Terms and Conditions (https://onlinelibrary.wiley.com/terms-and-conditions) on Wiley Online Library for rules of use; OA articles are governed by the applicable Creative Commons License

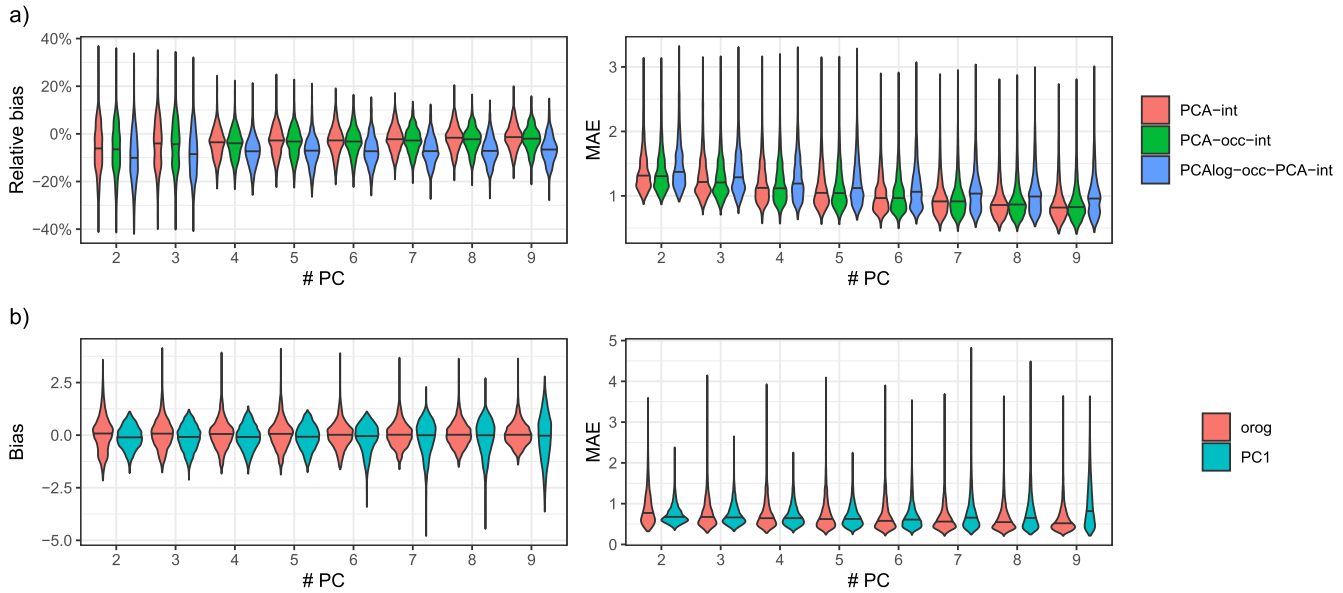


FIGURE 3 | Evaluation of the PCA-based downscaling using the perfect model setup (i.e., downscaling performed on upscaled observations and evaluated with the actual observations). Shown are violin density plots of (relative) bias and mean absolute error (MAE) with their median (solid line). (a) Precipitation in summer (JJA, June–August); PCA-int is a single component model, PCA-occ-int is a two-component model, one component is occurrence and the other is intensity, PCAlog-occ-PCA-int also has two separate components but uses fields from the logistic PCA for occurrence. (b) Daily minimum temperature; orog means that PC1 has been exchanged with an upscaled elevation field, while PC1 means that PC1 has been kept.

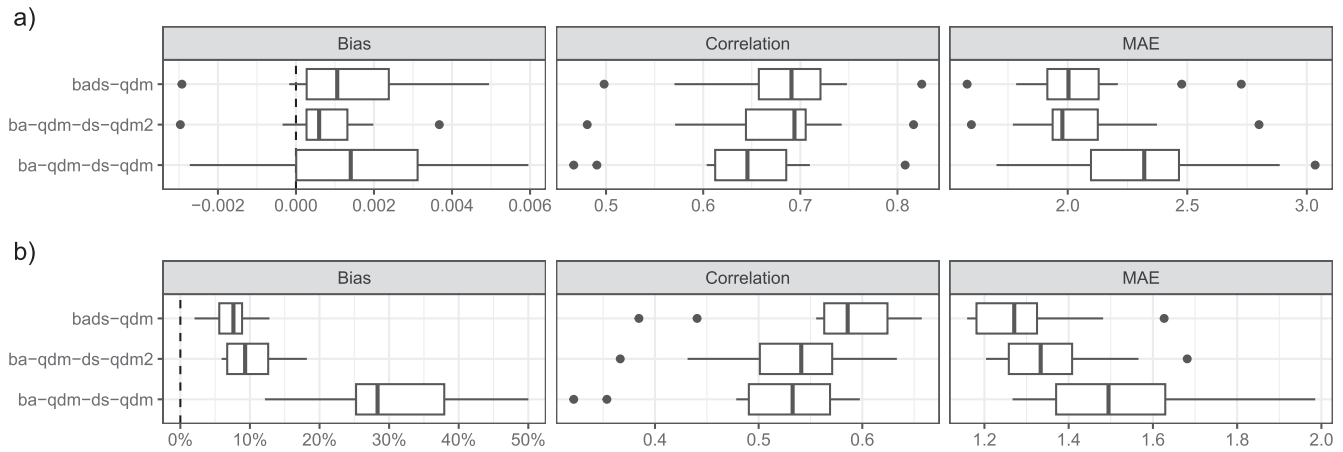


FIGURE 4 | Domain-averaged summary evaluation metrics for bias adjustment and downscaling of (a) winter minimum temperature (tasmin) and (b) winter precipitation (pr). Boxplots summarise the 11 RCMs considered in the present study.

seems to be no advantage in separating the bias adjustment from downscaling (*ba-qdm-ds-qdm*, *ba-qdm-ds-qdm2*) compared to performing a combined approach (*bads-qdm*). On the contrary, especially for precipitation, the combined approach yields better performance metrics (Figures 4b and S16). Moreover, when bias adjustment and downscaling are performed separately, using the same years for both steps (*ba-qdm-ds-qdm*) introduces much higher errors, especially for precipitation, than when different years are used in each step (*ba-qdm-ds-qdm2*).

4.3 | Evaluation of Different Downscaling Methods

Spatially-averaged metrics differed slightly among the downscaling methods. The quantile-based methods (*ba-qdm-ds-qdm2*, *bads-qdm*) were unbiased for summer maximum temperature (Figure 5a). The other downscaling methods performed similarly well: *ba-qdm-ds-pcalm* showed a −0.07°C bias for summer tasmax, *ba-qdm-ds-lr* 0.18°C and only *ba-qdm-ds-gam* had a larger range of domain-averaged biases (− 0.16,0.16). Correlations and MAE did not differ substantially between DS methods.

For summer precipitation (Figure 5b), the quantile-based methods (*ba-qdm-ds-qdm2*, *bads-qdm*) showed very little positive bias (< 5%, except for one RCM). On the other hand, *ba-qdm-ds-pcalm* had mostly negative biases, but in a similar range with the quantile-based methods (again mostly < 5%, except for one RCM outlier). Domain-averaged correlations did not differ among methods. However, the MAE of *ba-qdm-ds-pcalm*, 3.8 (range: 3.5, 4.4), was slightly lower than 3.9 (3.5, 4.3) for *ba-qdm-ds-qdm2* and 3.9 (3.5, 4.5) for *bads-qdm*.

10970088, 2026, 13, Downloaded from https://rmets.onlinelibrary.wiley.com/doi/10.1002/joc.70545 by CochraneItalia, Wiley Online Library on [03/11/2026]. See the Terms and Conditions (https://onlinelibrary.wiley.com/terms-and-conditions) on Wiley Online Library for rules of use; OA articles are governed by the applicable Creative Commons License

Results for the other seasons and minimum temperatures did not differ (Figures S14–S16). *ba-qdm-ds-qdm2* and *bads-qdm* had better metrics for temperature variables, while *ba-qdm-ds-pcalm* had minimally better MAE for precipitation.

Domain-averaged metrics can mask substantial information as errors across space can cancel each other out. This was particularly the case for temperature for *ba-qdm-ds-gam* and *ba-qdm-ds-pcalm* and to a lesser extent for *ba-qdm-ds-lr*. *ba-qdm-ds-gam* and *ba-qdm-ds-pcalm* had elevation-dependent biases, namely negative biases at high elevation and positive biases at low elevations (see Figure 6 for maximum temperatures in spring; with similar results for the other seasons, see Figure S17). Biases of *ba-qdm-ds-lr* were much lower and did not show a clear elevation dependency across the whole domain, but some elevation-related patterns for each gridcell. On the other hand, *ba-qdm-ds-qdm2* and *bads-qdm* had zero bias across the whole domain. MAE was extremely high for the lowest elevations for *ba-qdm-ds-gam*. *ba-qdm-ds-pcalm* showed higher MAE at both the highest and lowest elevations, while the other methods did not show particular spatial features for MAE. Correlations also depended on elevation and were generally lower for higher elevations across all methods, but particularly for *ba-qdm-ds-gam* and *ba-qdm-ds-pcalm*.

Spatial metrics for precipitation showed different results compared to temperature (see Figure 7 for spring). For precipitation, the quantile-based methods also showed biases of $(-3\%, 6\%)$ for *bads-qdm* and $(0\%, 10\%)$ for *ba-qdm-ds-qdm2*. *ba-qdm-ds-pcalm* had a bias range of −20% to 20%. MAE and correlations showed similar spatial patterns across methods, with higher

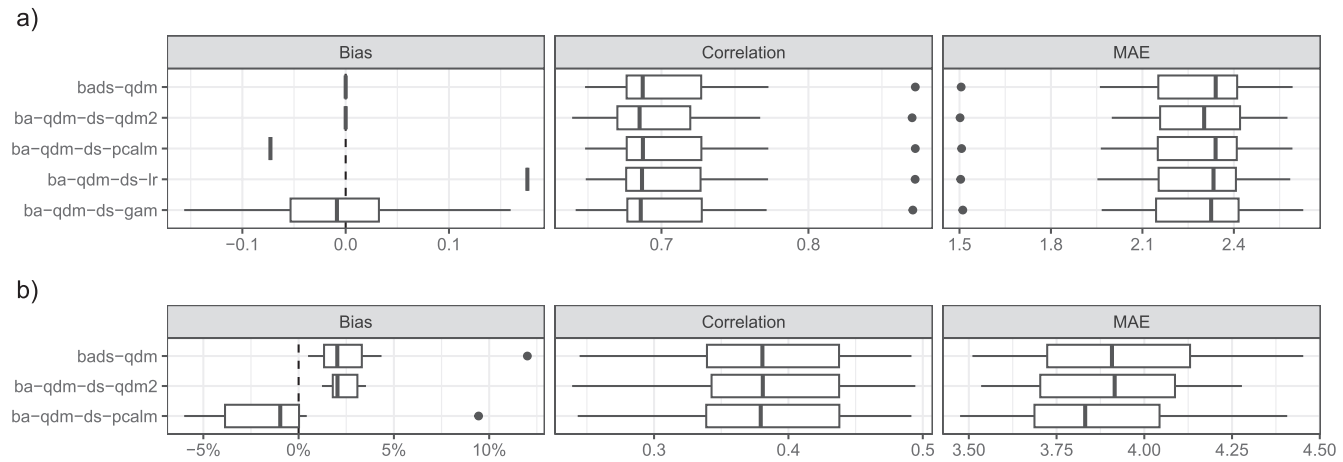


FIGURE 5 | Spatially-averaged summary evaluation metrics for bias adjustment and downscaling of (a) summer maximum temperature (tasmax) and (b) summer precipitation (pr). Boxplots summarise the 11 RCMs considered in the present study.

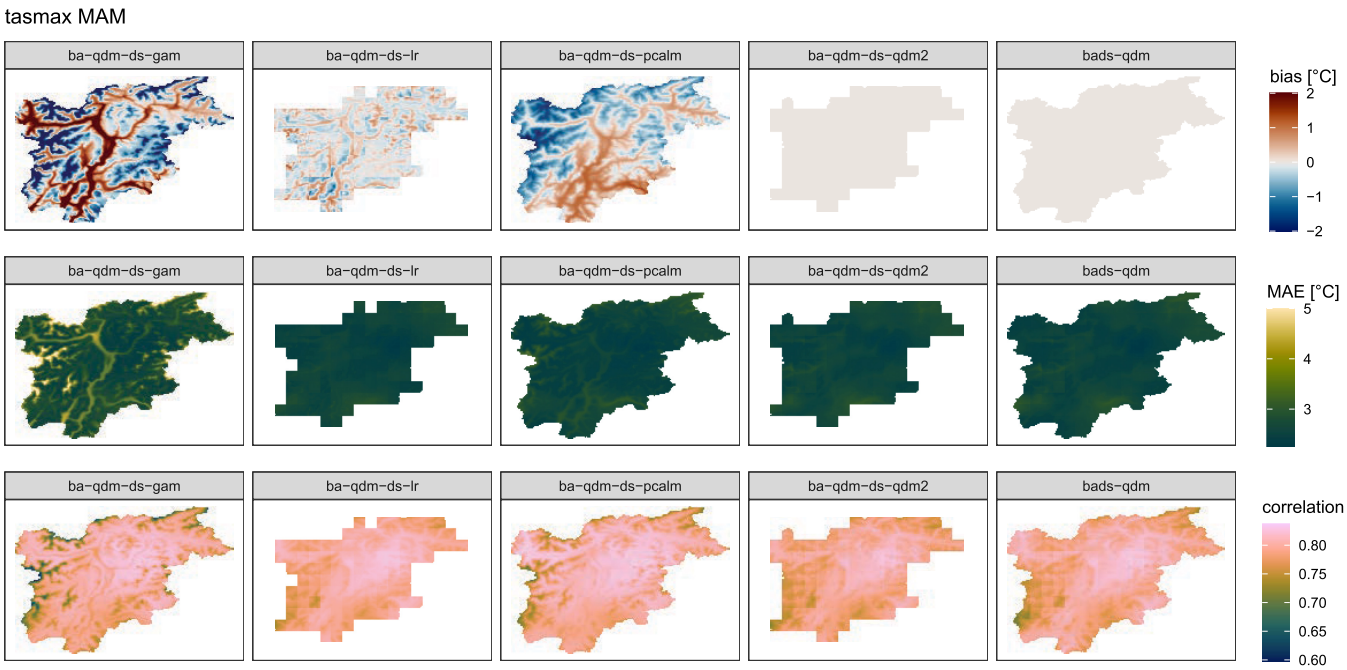


FIGURE 6 | RCM ensemble average metrics for maximum temperature in spring. For bias the colour scale range has been capped to (−2,2) and all values below/above are shown with the same colour as −2 and 2. Similarly, MAE has been capped to a maximum of 5.

10970088, 2026, 13, Downloaded from https://rmets.onlinelibrary.wiley.com/doi/10.1002/joc.70545 by CochraneItalia, Wiley Online Library on [03/11/2026]. See the Terms and Conditions (https://onlinelibrary.wiley.com/terms-and-conditions) on Wiley Online Library for rules of use; OA articles are governed by the applicable Creative Commons License

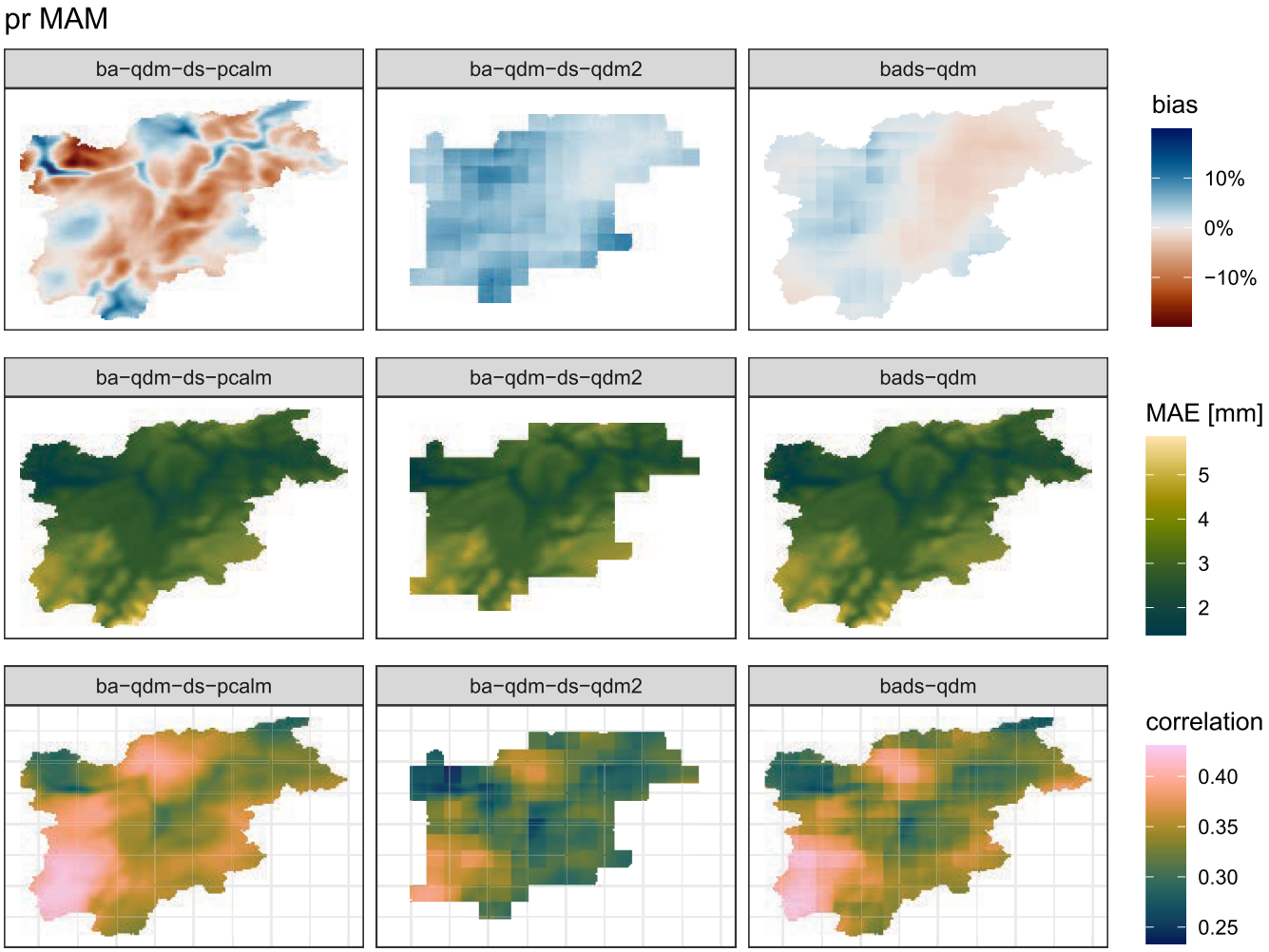


FIGURE 7 | RCM ensemble average metrics for spring precipitation.

MAE in the south of the study area and higher correlations in the south-east.

The other seasons, as well as minimum temperatures, showed similar patterns regarding the spatial metrics (Figures S17 and S18).

4.4 | Multivariate Versus Univariate

Snowfall metrics showed contrasting results on the benefit of multivariate bias adjustment that differed between seasons, downscaling methods and evaluation metrics (Figure 8). For instance, MAE is consistently higher and correlations are lower for the multivariate variant of each BA-DS combination, while biases differ between seasons and methods. In winter, for the combined BA-DS the univariate *bads-qdm* has a better median bias of −2% compared to the multivariate *bads-mbcn* with 4%; however, the spatial distribution of errors is narrower for *bads-mbcn*, though it is skewed towards positive biases. For the PCA-based downscaling, the univariate *ba-qdm-ds-pcalm* has a larger median bias of −2% compared to the multivariate *ba-mbcn-ds-pcalm* with 0% and again the multivariate variant has a slightly narrower error distribution. In spring, the multivariate variants have better bias than univariate variants, especially *bads-mbcn* is now unbiased with a narrow bias distribution, while *ba-mbcn-ds-dspcalm* improves on median bias compared to the univariate variant (−8% versus −18%), but its error distribution is still wider than for *bads-mbcn*.

4.5 | Other Aspects: Spatial Features and Extremes

While the previous sections addressed the main study objectives, here we present ancillary results on downscaling, particularly regarding spatial issues and extremes.

4.5.1 | Spatial Correlation

PCA-based downscaling shows consistently better performance from a spatial point of view. The correlations between spatial fields were the highest for all seasons and all variables (Figure S19). This is not a surprise, since *ba-qdm-ds-pcalm* is a spatial downscaling method and the PCA-derived spatial fields used in the downscaling are estimated from the observed maps. Conversely, for the quantile-based methods with the cell-by-cell application, the spatial fields are coarse, in addition to the gridcell boundary effects of the equally coarse resolution input. Consequently, this analysis highlights the better performance

10970088, 2026, 13, Downloaded from https://rmets.onlinelibrary.wiley.com/doi/10.1002/joc.70545 by CochraneItalia, Wiley Online Library on [03/11/2026]. See the Terms and Conditions (https://onlinelibrary.wiley.com/terms-and-conditions) on Wiley Online Library for rules of use; OA articles are governed by the applicable Creative Commons License

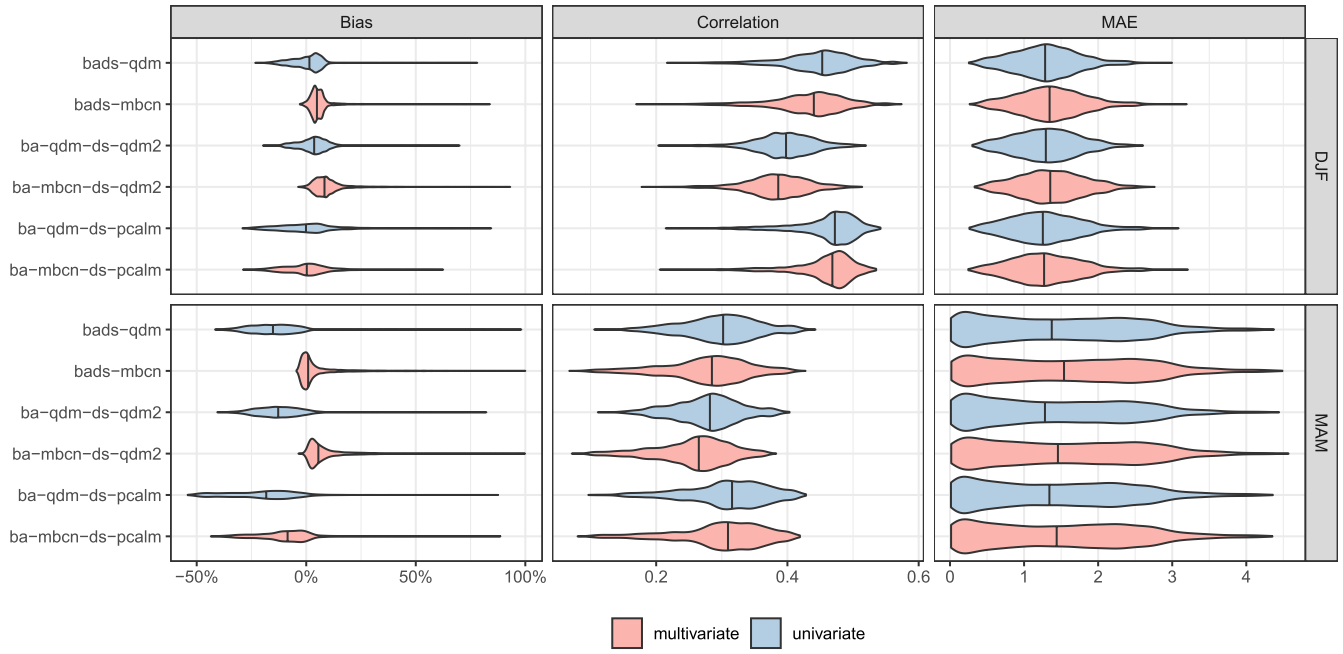


FIGURE 8 | Ensemble-averaged evaluation metrics for the multivariate snowfall index. Violin density plots summarise the gridcells.

in the spatial domain of the PCA-based downscaling compared to a quantile mapping performed cell-by-cell. For example, in the univariate case, the average correlation in space of winter tasmin was 0.93 for *ba-qdm-ds-pcalm* and 0.88 for *bads-qdm*. Precipitation had generally lower correlations, but also here *ba-qdm-ds-pcalm* had the highest values; for example, in winter, 0.29 compared to 0.22 for *bads-qdm*.

Moreover, the correlations in space were consistently lower for the multivariate BA compared to the univariate BA (Figure S19). While this is true for the quantile-based methods, for temperature, the PCA-based downscaling showed almost no differences between multivariate and univariate BA. The reason for this is that multivariate BA reshuffles values in time to match inter-variable correlations. In the case of simultaneous BA&DS (*bads-mbcn*), this is most clearly seen as 'speckle patterns' (Figure S20), while this high-resolution speckle was not observed when the DS step was separated from the BA (*ba-mbcn-ds-qdm2*). Nevertheless, the temporal reshuffling at the BA step (at RCM scale), although less evident than the high-resolution speckles, still reduces the coherence in the spatial domain for DS.

4.5.2 | Extremes

The downscaling errors increase at the tails of the seasonal distribution, more so for temperature than for precipitation. For example, ensemble-averaged biases of tasmin in winter for *bads-mbcn* are nearly unbiased for average conditions with a median bias over all gridcells of 0.1°C (range −0.1, 0.4), compared to −0.8°C (−2.3, −0.0) for the 1st percentile and −2.3°C (−4.8, 0.8) for the absolute minima (Figure S21). For percentiles above the median, biases are positive instead of negative, for example, 0.2°C (−0.3, 0.7) for the 99th percentile and 1.0°C (−0.7, 2.2) for the absolute maxima. Similar conclusions are valid for the other seasons or for tasmax (Figure S22). For precipitation, biases up to the 99th percentile are very similar to means, only for the absolute maxima they reach very high values regardless of season (Figure S23). For instance, summer precipitation maxima *bads-mbcn* shows a median bias of 50% over all gridcells that can reach up to 114% for certain gridcells.

5 | Discussion

5.1 | PCA-Based and Spatial Downscaling

Spatial downscaling is a fairly new research topic. While multi-site weather generators existed for a longer time (see, e.g., Dubrovsky et al. 2020 and references therein), there has been very little progress on spatial fields or grids in general (Maurer et al. 2010), except for the sub-optimal gridcell-by-gridcell application of quantile mapping or other techniques, such as in, for example, Fischer et al. (2022). The spatial extensions of multivariate techniques were found to be not computationally robust in a high-dimensional setting such as the one in our study (François et al. 2020). Recently, the advent of deep learning and especially convolutional neural networks with their inherent capability to model spatial features, seems to be a promising path (Baño-Medina et al. 2022), even though their application in a climate projection setting with temporal asynchrony in the historical training poses some challenges, as the training has to be performed with reanalysis which might not be representative for GCMs (Manzanas et al. 2015). Nonetheless, deep learning has been shown to successfully emulate dynamical downscaling (Tomasi et al. 2025).

Our proposed approach that is based on PCA-derived spatial fields showed very promising results for spatial downscaling, especially for precipitation. There were issues with this approach for temperature, most likely due to the strong elevation dependency of temperature, along with the mismatch between the real and smoothed model orography. Consequently, the statistical

10970088, 2026, 13, Downloaded from https://rmets.onlinelibrary.wiley.com/doi/10.1002/joc.70545 by CochraneItalia, Wiley Online Library on [03/11/2026]. See the Terms and Conditions (https://onlinelibrary.wiley.com/terms-and-conditions) on Wiley Online Library for rules of use; OA articles are governed by the applicable Creative Commons License

methods need to extrapolate beyond the elevation coverage of the climate models, which can introduce large statistical artefacts, which were also evident in the GAM interpolation method (*ba-qdm-ds-gam*). Moreover, our approach assumes a linear relationship for each PC, which is expected to hold over the whole domain. Since the first PC for temperature is related to elevation, this implies a linear lapse rate over the whole domain, which is unlikely to be accurate. However, the alternative of using non-linear relationships (e.g., with GAMs) might place too much emphasis on the RCM coarse-resolution elevation profile, which may not be representative of the high-resolution elevation profile. Consequently, quantile-based approaches are more flexible in modelling the relationship between coarse and fine scales and thus show superior results for temperature.

For precipitation, the PCA-based downscaling showed very good results, better than those obtained by the quantile-based methods. Moreover, it produced the most realistic spatial precipitation fields, as shown in some example maps (Figure S24). Consequently, we see promising future applications of the PCA-based downscaling, especially in domains where spatial coherence is important, such as hydrological modelling.

The PCA-based approach strongly relies on the input data and replicates the patterns in the observations. For instance, the second PC shows a distinct region of very low values in the NE corner of the domain (Figure S7), which is most pronounced in minimum temperatures during DJF and SON. But also for the other seasons and for temperature maxima, we observed a gradient between the NE and SW of the domain. We attribute this to a climatological behaviour influenced by the main ridge of the Alps bordering the North; however, it might also be affected by boundary issues at the edge of the domain of the observational dataset.

5.2 | Bias Adjustment and Downscaling

In separating bias adjustment from downscaling, we found contrasting results. On the one hand, separating them reduces undesired effects such as the speckle found in *bads-mbcn* (Figure S20). On the other, joint bias adjustment and downscaling generally improve metrics. However, separating BA from DS allows for choosing different methods for each step, for instance, combining QDM for BA with a PCA-based DS, as performed in our study. Also, one could imagine using a simple univariate approach for DS but a complex multivariate approach for BA, potentially also including spatial or temporal correlations, since it is performed at the coarse resolution and thus requires less computational power and has less chances to produce computational artefacts, as reported, for example, by François et al. (2020).

It has been argued in the literature that quantile mapping methods should not be used to perform downscaling because, at least in the case of precipitation, quantile mapping cannot account for small-scale spatial processes and, in the case of non-trend preserving methods, trends can be artificially deteriorated (Maraun 2013). Thus, it was suggested to use quantile mapping methods only for bias adjustment at the same scale of the climate model output (Maraun 2016; Maraun et al. 2019). This recommendation has been adopted, for example, in Lange (2019), however, we are not aware of any studies that explicitly examined the separation of bias adjustment and downscaling with quantile mapping methods. Based on the findings in our study, we cannot provide clear recommendations on separating BA and DS, but we argue that it warrants further research.

Table 3 provides a synthesis of the advantages and disadvantages of the different downscaling methods considered in this study. Our study further corroborates the use of quantile mapping methods in climate model post-processing and bias adjustment. Even in a cross-validation approach with only 10 years of training data, QDM can reproduce basic climatological features with almost zero bias. This is in line with previous studies showing better performance of quantile mapping methods compared to parametric or other approaches (Gutiérrez et al. 2019). However, we did not explicitly test the impact of the number of training years on the performance. The results for *ba-qdm-ds-qdm*, where the same years have been used in the BA and the DS step, highlight a potentially strong error source of the choice of training period. However, Reder et al. (2025) tested the impact of different 10-year slices

TABLE 3 | Summary of the pros and cons of the univariate downscaling methods analysed in this study.

DS method	Pro	Con
bads-qdm	+ high accuracy overall	– RCM cell boundary artefacts
ba-qdm-ds-qdm, *ba-qdm-ds-qdm2*	+ allows to combine different BA and DS methods	– generally lower accuracy than simultaneous BA and DS – needs different training periods for BA and DS – RCM cell boundary artefacts
ba-qdm-ds-pcalm	+ high accuracy for precipitation + highest spatial coherence	– accuracy for temperature differs a lot by RCM
ba-qdm-ds-lr	+ easy to use + good accuracy + no need for observations/reference data	– only temperature – RCM cell boundary artefacts
ba-qdm-ds-gam	+ no need for observations/reference data + smooth spatial fields	– poor performance, especially when extrapolating beyond elevation range of RCM – only temperature

10970088, 2026, 13, Downloaded from https://rmets.onlinelibrary.wiley.com/doi/10.1002/joc.70545 by CochraneItalia, Wiley Online Library on [03/11/2026]. See the Terms and Conditions (https://onlinelibrary.wiley.com/terms-and-conditions) on Wiley Online Library for rules of use; OA articles are governed by the applicable Creative Commons License

on quantile mapping as a downscaling tool and found only a minor effect of the choice of years. They further argued that these differences should become minimal if the training period achieves climate scales (> 20 years).

5.3 | Multivariate vs. Univariate

Multivariate bias adjustment has been tested extensively in the literature, with some studies showing no clear recommendation for using multivariate methods (Tootoonchi et al. 2022; François et al. 2020; Meyer et al. 2019) and others highlighting the strengths of multivariate approaches (Vrac and Friederichs 2015; Eum et al. 2020; Cannon 2016). Astagneau et al. (2025) tested multivariate bias adjustment at the RCM scale in a single-model large-ensemble setup and further used a hydrological model to validate results. They found no benefit of multivariate approaches, neither in snow water equivalent nor in runoff and advise against using them, since they can degrade other features, such as spatial or temporal aspects. Astagneau et al. (2025) argue that their climate model showed correlations between temperature and precipitation similar to those observed, so these correlations were inherited in the univariate approach, making a multivariate adjustment unnecessary. We analysed the correlations between temperature and precipitation for the 11 RCMs used in our study and found that some RCMs reproduced observed correlations well and others not (Figure S25). We argue that multivariate adjustments are more useful when the RCMs do not reproduce observed correlations, since after the multivariate adjustment, all RCMs showed correlations similar to observations (Figure S25).

In our study, we found minor benefits from using a multivariate approach. However, we only used a simple meteorological index to evaluate the benefits of multivariate bias adjustment. Potentially different results could arise if more elaborated tools or impact models are used, such as hydrological models. For instance, Allard et al. (2025) assessed the impact of multivariate adjustments in various impact models, including simple single-variable and complex multi-variable models, such as phenological stage, evapotranspiration, soil water content and fire weather risk. They found great improvements in using multivariate approaches when the considered impact model is multivariate. But also in Allard et al. (2025), the authors argue that the univariate approach performs well and is a safe option, since it inherits the properties of the GCM or RCM, which can already be good, similar to the hypothesis of Astagneau et al. (2025). Allard et al. (2025) further tested different bias adjustment methods and configurations adjusting inter-variable, spatial and temporal correlations. They concluded that there is no best multivariate bias adjustment method and that accounting for certain correlations might degrade others. This is in line to our findings, where we only adjusted the inter-variable correlations and lost performance in the spatial domain (Figure S19).

5.4 | Other

Downscaling extremes is always challenging, not only for model-output statistics, such as quantile mapping, but also in general for any statistical downscaling (Hertig et al. 2019). Note that this is also true for dynamical downscaling and especially for precipitation, for example, in terms of predicting accumulated total precipitation or the location of extremes (Bettolli et al. 2021). We hypothesise that the differences we observed for the most extreme quantiles (Figures S21–S23) emerge at the bias adjustment step, since the results are almost identical to the ones obtained by looking at the extremes from the bias adjustment at the RCM resolution (Figure S26).

Quantile-based methods are often used in downscaling and bias adjustment to provide climate information and they are especially used for calculating climate indices of extremes. However, we found high errors (overestimation) for extremes, similar to previous studies (Haylock et al. 2006; Casanueva et al. 2018; Hertig et al. 2019). Consequently, caution is required when providing quantile-mapped data for users who need to calculate extremes. In this regard, parametric or semi-parametric variants might be better suited to account for tail behaviour (Switanek et al. 2017; Tani and Gobiet 2019), especially for precipitation, where the most extreme quantiles strongly depend on the sampling period.

Except for biases of temperatures, all other metrics and other variables showed considerable variations among the RCMs (see the range of boxplots in Figures S14–S16). This variability between RCMs was often higher than the difference between downscaling methods. For tasmax in winter, SMHI-RCA4 was a negative outlier in terms of correlations and MAE; in spring and fall, IPSL-WRF381P, while CLMcom-CCLM4-8-17 was a positive outlier, especially in summer and autumn, but also for winter tasmin. Regarding pr, CNRM-ALADIN63 showed higher biases than the other models in summer; IPSL-WRF381P showed a higher MAE in spring; and IPSL-WRF381P and ICTP-RegCM4-6 had the lowest correlations in winter.

6 | Conclusions

We proposed a new spatial statistical downscaling method based on PCA, which showed, for precipitation, performance similar to or better than that of the widely used quantile delta mapping. This method extends the statistical downscaling to include spatial information, which is an important aspect for future impact studies that require spatial coherence, for instance, snow simulations or hydrological modelling. The PCA-based downscaling is versatile and can be applied wherever high-resolution gridded data is available.

Separating bias adjustment from downscaling showed worse performance than the combined bias adjustment and downscaling when quantile delta mapping was used in both cases. In the multivariate case, however, the separation has some benefit, as it does not create the noisy speckle observed in simultaneous BA&DS. And the separation allows for different approaches to be combined in BA and DS. Nonetheless, this topic still requires further research.

Multivariate bias adjustment showed a minor benefit over univariate adjustment in our study. However, we only used

10970088, 2026, 13, Downloaded from https://rmets.onlinelibrary.wiley.com/doi/10.1002/joc.70545 by CochraneItalia, Wiley Online Library on [03/11/2026]. See the Terms and Conditions (https://onlinelibrary.wiley.com/terms-and-conditions) on Wiley Online Library for rules of use; OA articles are governed by the applicable Creative Commons License

a simplistic snowfall index to capture inter-variable correlations, which, anyway, are rather low for temperature and precipitation in our study area. Benefits of multivariate adjustment might be clearer after applying more complex impact models (similar to the spirit of Allard et al. 2025). Arguably, as climate modelling moves to high spatial (< 2 km) and temporal scales (1 h), for example, using convection-resolving models, then the benefits of multivariate BA might become even more apparent. Moreover, the inclusion of further variables could also alter the results, for example, humidity or radiation as they have a very strong correlation to temperature and precipitation.

Unlike many previous studies, we used a multi-model ensemble rather than a single model. We recommend this approach, especially for assessing multivariate bias adjustment, since models showed different performance in reproducing the inter-variable correlations. Hence, more robust conclusions can be drawn that do not depend on a single climate model. Finally, our study used reanalysis-driven climate models; future studies could also examine results from applying the methods to GCM-driven climate projections.

Author Contributions

Anna Napoli: methodology, data curation, writing – review and editing. **Michael Matiu:** conceptualization, methodology, data curation, software, formal analysis, visualization, writing – original draft, writing – review and editing. **Bruno Majone:** conceptualization, methodology, supervision, writing – review and editing, funding acquisition. **Alberto Bellin:** methodology, conceptualization, supervision, writing – review and editing, funding acquisition. **Dino Zardi:** methodology, funding acquisition, writing – review and editing, supervision.

Acknowledgements

We thank Alice Crespi for the provision of the observational data interpolated directly to the 1 km grid including minimum and maximum daily temperatures and precipitation. Open access publishing facilitated by Universita degli Studi di Trento, as part of the Wiley - CRUI-CARE agreement.

This research received financial support from the project 'Sintesi degli studi sui cambiamenti climatici e i loro impatti ed elaborazione di scenari climatici di riferimento per il Trentino' funded by the Agency for Environmental Protection (Agenzia Provinciale per la Protezione dell'Ambiente, APPA) of the Autonomous Province of Trento, Italy. Further funding came from the European Union—NextGenerationEU, PRIN 2022 PNRR (Prot. no. P20227NPLW, CUP E53D23021860001). A.N. has been supported by "Fondazione CARITRO" (Cassa di Risparmio di Trento e Rovereto) within the project "Insight into the physical mechanisms underlying convection phenomena for a better understanding of its future evolution in the context of climate change in the Trentino region". A.B. and B.M. acknowledge the Italian Ministry of Universities and Research (MUR), in the framework of the project DICAM-EXC (Departments of Excellence 2023-2027, grant L232/2016). D.Z., A.B. and B.M. acknowledge support from the "iNEST (Interconnected Nord-Est Innovation Ecosystem)" project funded by the European Union under NextGenerationEU (PNRR, Mission 4.2, Investment 1.5, Project ID: ECS 00000043).

Funding

This work was supported by the Agency for Environmental Protection of the Autonomous Province of Trento, Italy. European Commission, NextGenerationEU, PRIN2022 PNRR (Prot. no. P20227NPLW), NextGenerationEU (PNRR, Mission 4.2, Investment 1.5). Fondazione Cassa Di Risparmio Di Trento E Rovereto.

Conflicts of Interest

The authors declare no conflicts of interest.

Data Availability Statement

All code used in the analysis will be made available under https://github.com/tnclima/downscaling. Since the produced data exceeds reasonable limits for open repositories, it will only be made available upon request. Sources of the input data can be found in the Section 3.

References

Adler, C., P. Wester, I. Bhatt, et al. 2022. "Cross-Chapter Paper 5: Mountains." In *Climate Change 2022: Impacts, Adaptation and Vulnerability. Contribution of Working Group II to the Sixth Assessment Report of the Intergovernmental Panel on Climate Change*, edited by H. O. Pörtner, D. C. Roberts, M. Tignor, et al., 2273–2318. Cambridge University Press.

Allard, D., M. Vrac, B. François, and I. García de Cortázar-Atauri. 2025. "Assessing Multivariate Bias Corrections of Climate Simulations on Various Impact Models Under Climate Change." *Hydrology and Earth System Sciences* 29, no. 18: 4711–4738. https://doi.org/10.5194/hess-29-4711-2025.

Astagneau, P. C., R. R. Wood, M. Vrac, et al. 2025. "Impact of Bias Adjustment Strategy on Ensemble Projections of Hydrological Extremes." *Hydrology and Earth System Sciences* 29, no. 20: 5695–5718. https://doi.org/10.5194/hess-29-5695-2025.

Ban, N., C. Caillaud, E. Coppola, et al. 2021. "The First Multi-Model Ensemble of Regional Climate Simulations at Kilometer-Scale Resolution, Part I: Evaluation of Precipitation." *Climate Dynamics* 57, no. 1: 275–302. https://doi.org/10.1007/s00382-021-05708-w.

Baño-Medina, J., R. Manzanas, E. Cimadevilla, et al. 2022. "Downscaling Multi-Model Climate Projection Ensembles With Deep Learning (DeepESD): Contribution to CORDEX EUR-44." *Geoscientific Model Development* 15, no. 17: 6747–6758. https://doi.org/10.5194/gmd-15-6747-2022.

Berthou, S., E. J. Kendon, S. C. Chan, et al. 2020. "Pan-European Climate at Convection-Permitting Scale: A Model Intercomparison Study." *Climate Dynamics* 55, no. 1: 35–59. https://doi.org/10.1007/s00382-018-4114-6.

Bettolli, M. L., S. A. Solman, R. P. da Rocha, et al. 2021. "The CORDEX Flagship Pilot Study in Southeastern South America: A Comparative Study of Statistical and Dynamical Downscaling Models in Simulating Daily Extreme Precipitation Events." *Climate Dynamics* 56, no. 5: 1589–1608. https://doi.org/10.1007/s00382-020-05549-z.

Cannon, A. J. 2016. "Multivariate Bias Correction of Climate Model Output: Matching Marginal Distributions and Intervariable Dependence Structure." *Journal of Climate* 29, no. 19: 7045–7064. https://doi.org/10.1175/JCLI-D-15-0679.1.

Cannon, A. J. 2018. "Multivariate Quantile Mapping Bias Correction: An N-Dimensional Probability Density Function Transform for Climate Model Simulations of Multiple Variables." *Climate Dynamics* 50, no. 1: 31–49. https://doi.org/10.1007/s00382-017-3580-6.

Cannon, A. J. 2023. "MBC: Multivariate Bias Correction of Climate Model Outputs." R Package Version 0.10-6. https://CRAN.R-project.org/package=MBC.

Cannon, A. J., S. R. Sobie, and T. Q. Murdock. 2015. "Bias Correction of GCM Precipitation by Quantile Mapping: How Well Do Methods Preserve Changes in Quantiles and Extremes?" *Journal of Climate* 28, no. 17: 6938–6959. https://doi.org/10.1175/JCLI-D-14-00754.1.

10970088, 2026, 13, Downloaded from https://rmets.onlinelibrary.wiley.com/doi/10.1002/joc.70545 by CochraneItalia, Wiley Online Library on [03/11/2026]. See the Terms and Conditions (https://onlinelibrary.wiley.com/terms-and-conditions) on Wiley Online Library for rules of use; OA articles are governed by the applicable Creative Commons License

Casanueva, A., J. Bedia, S. Herrera, J. Fernández, and J. M. Gutiérrez. 2018. "Direct and Component-Wise Bias Correction of Multi-Variate Climate Indices: The Percentile Adjustment Function Diagnostic Tool." *Climatic Change* 147, no. 3: 411–425. https://doi.org/10.1007/s10584-018-2167-5.

Casanueva, A., S. Herrera, J. Fernández, and J. Gutiérrez. 2016. "Towards a Fair Comparison of Statistical and Dynamical Downscaling in the Framework of the EURO-CORDEX Initiative." *Climatic Change* 137, no. 3: 411–426. https://doi.org/10.1007/s10584-016-1683-4.

Coppola, E., R. Nogherotto, J. M. Ciarlo', et al. 2021. "Assessment of the European Climate Projections as Simulated by the Large EURO-CORDEX Regional and Global Climate Model Ensemble." *Journal of Geophysical Research: Atmospheres* 126, no. 4: e2019JD032356. https://doi.org/10.1029/2019JD032356.

Crespi, A., M. Matiu, G. Bertoldi, M. Petitta, and M. Zebisch. 2021. "A High-Resolution Gridded Dataset of Daily Temperature and Precipitation Records (1980–2018) for Trentino-South Tyrol (North-Eastern Italian Alps)." *Earth System Science Data* 13, no. 6: 2801–2818. https://doi.org/10.5194/essd-13-2801-2021.

de Vries, H., G. Lenderink, and E. van Meijgaard. 2014. "Future Snowfall in Western and Central Europe Projected With a High-Resolution Regional Climate Model Ensemble." *Geophysical Research Letters* 41, no. 12: 4294–4299. https://doi.org/10.1002/2014GL059724.

Dubrovsky, M., R. Huth, H. Dabhi, and M. W. Rotach. 2020. "Parametric Gridded Weather Generator for Use in Present and Future Climates: Focus on Spatial Temperature Characteristics." *Theoretical and Applied Climatology* 139, no. 3: 1031–1044. https://doi.org/10.1007/s00704-019-03027-z.

Eum, H. I., A. Gupta, and Y. Dibike. 2020. "Effects of Univariate and Multivariate Statistical Downscaling Methods on Climatic and Hydrologic Indicators for Alberta, Canada." *Journal of Hydrology* 588: 125065. https://doi.org/10.1016/j.jhydrol.2020.125065.

Fischer, A. M., K. M. Strassmann, M. Croci-Maspoli, et al. 2022. "Climate Scenarios for Switzerland CH2018 – Approach and Implications." *Climate Services* 26: 100288. https://doi.org/10.1016/j.cliser.2022.100288.

Fosser, G., M. Gaetani, E. J. Kendon, et al. 2024. "Convection-Permitting Climate Models Offer More Certain Extreme Rainfall Projections." *npj Climate and Atmospheric Science* 7, no. 1: 51. https://doi.org/10.1038/s41612-024-00600-w.

Fowler, H. J., S. Blenkinsop, and C. Tebaldi. 2007. "Linking Climate Change Modelling to Impacts Studies: Recent Advances in Downscaling Techniques for Hydrological Modelling." *International Journal of Climatology* 27, no. 12: 1547–1578. https://doi.org/10.1002/joc.1556.

François, B., M. Vrac, A. J. Cannon, Y. Robin, and D. Allard. 2020. "Multivariate Bias Corrections of Climate Simulations: Which Benefits for Which Losses?" *Earth System Dynamics* 11, no. 2: 537–562. https://doi.org/10.5194/esd-11-537-2020.

Frei, C., M. Willi, R. Stöckli, and B. Dürr. 2015. "Spatial Analysis of Sunshine Duration in Complex Terrain by Non-Contemporaneous Combination of Station and Satellite Data." *International Journal of Climatology* 35, no. 15: 4771–4790. https://doi.org/10.1002/joc.4322.

Frei, P., S. Kotlarski, M. A. Liniger, and C. Schär. 2018. "Future Snowfall in the Alps: Projections Based on the EURO-CORDEX Regional Climate Models." *Cryosphere* 12, no. 1: 1–24. https://doi.org/10.5194/tc-12-1-2018.

Geppert, C., A. Bertolli, F. Prosser, and L. Marini. 2023. "Red-Listed Plants Are Contracting Their Elevational Range Faster Than Common Plants in the European Alps." *Proceedings of the National Academy of Sciences of the United States of America* 120, no. 12: e2211531120. https://doi.org/10.1073/pnas.2211531120.

Giorgi, F. 2019. "Thirty Years of Regional Climate Modeling: Where Are we and Where Are we Going Next?" *Journal of Geophysical Research: Atmospheres* 124, no. 11: 5696–5723. https://doi.org/10.1029/2018JD030094.

Gutiérrez, J. M., D. Maraun, M. Widmann, et al. 2019. "An Intercomparison of a Large Ensemble of Statistical Downscaling Methods Over Europe: Results From the VALUE Perfect Predictor Cross-Validation Experiment." *International Journal of Climatology* 39, no. 9: 3750–3785. https://doi.org/10.1002/joc.5462.

Haylock, M. R., G. C. Cawley, C. Harpham, R. L. Wilby, and C. M. Goodess. 2006. "Downscaling Heavy Precipitation Over the United Kingdom: A Comparison of Dynamical and Statistical Methods and Their Future Scenarios." *International Journal of Climatology* 26, no. 10: 1397–1415. https://doi.org/10.1002/joc.1318.

Hertig, E., D. Maraun, J. Bartholy, et al. 2019. "Comparison of Statistical Downscaling Methods With Respect to Extreme Events Over Europe: Validation Results From the Perfect Predictor Experiment of the COST Action VALUE." *International Journal of Climatology* 39, no. 9: 3846–3867. https://doi.org/10.1002/joc.5469.

Hiebl, J., Q. Bourgeois, A. M. Tilg, and C. Frei. 2024. "Daily Sunshine Grids for Austria Since 1961 – Combining Station and Satellite Observations for a Multi-Decadal Climate-Monitoring Dataset." *Theoretical and Applied Climatology* 155, no. 8: 8337–8360. https://doi.org/10.1007/s00704-024-05103-5.

Hock, R., G. Rasul, C. Adler, et al. 2019. "High Mountain Areas." In *IPCC Special Report on the Ocean and Cryosphere in a Changing Climate*, edited by H. O. Pörtner, D. Roberts, V. Masson-Delmotte, et al. Cambridge University Press.

Jacob, D., J. Petersen, B. Eggert, et al. 2014. "EURO-CORDEX: New High-Resolution Climate Change Projections for European Impact Research." *Regional Environmental Change* 14, no. 2: 563–578. https://doi.org/10.1007/s10113-013-0499-2.

Kotlarski, S., D. Lüthi, and C. Schär. 2015. "The Elevation Dependency of 21st Century European Climate Change: An RCM Ensemble Perspective." *International Journal of Climatology* 35, no. 13: 3902–3920. https://doi.org/10.1002/joc.4254.

Landgraf, A. J., and Y. Lee. 2020. "Dimensionality Reduction for Binary Data Through the Projection of Natural Parameters." *Journal of Multivariate Analysis* 180: 104668. https://doi.org/10.1016/j.jmva.2020.104668.

Lange, S. 2019. "Trend-Preserving Bias Adjustment and Statistical Downscaling With ISIMIP3BASD (v1.0)." *Geoscientific Model Development* 12, no. 7: 3055–3070. https://doi.org/10.5194/gmd-12-3055-2019.

Liston, G. E., and K. Elder. 2006. "A Meteorological Distribution System for High-Resolution Terrestrial Modeling (MicroMet)." *Journal of Hydrometeorology* 7, no. 2: 217–234. https://doi.org/10.1175/JHM486.1.

Lucas-Picher, P., D. Argüeso, E. Brisson, et al. 2021. "Convection-Permitting Modeling With Regional Climate Models: Latest Developments and Next Steps." *WIREs Climate Change* 12, no. 6: e731. https://doi.org/10.1002/wcc.731.

Lüthi, S., N. Ban, S. Kotlarski, C. R. Steger, T. Jonas, and C. Schär. 2019. "Projections of Alpine Snow-Cover in a High-Resolution Climate Simulation." *Atmosphere* 10, no. 8: 463. https://doi.org/10.3390/atmos10080463.

Majone, B., F. Villa, R. Deidda, and A. Bellin. 2016. "Impact of Climate Change and Water Use Policies on Hydropower Potential in the South-Eastern Alpine Region." *Science of the Total Environment* 543: 965–980. https://doi.org/10.1016/j.scitotenv.2015.05.009.

Manzanas, R., S. Brands, D. San-Martín, A. Lucero, C. Limbo, and J. M. Gutiérrez. 2015. "Statistical Downscaling in the Tropics Can be Sensitive to Reanalysis Choice: A Case Study for Precipitation in The Philippines." *Journal of Climate* 28, no. 10: 4171–4184. https://doi.org/10.1175/JCLI-D-14-00331.1.

10970088, 2026, 13, Downloaded from https://rmets.onlinelibrary.wiley.com/doi/10.1002/joc.70545 by CochraneItalia, Wiley Online Library on [03/11/2026]. See the Terms and Conditions (https://onlinelibrary.wiley.com/terms-and-conditions) on Wiley Online Library for rules of use; OA articles are governed by the applicable Creative Commons License

Maraun, D. 2013. "Bias Correction, Quantile Mapping, and Downscaling: Revisiting the Inflation Issue." *Journal of Climate* 26, no. 6: 2137–2143. https://doi.org/10.1175/JCLI-D-12-00821.1.

Maraun, D. 2016. "Bias Correcting Climate Change Simulations - a Critical Review." *Current Climate Change Reports* 2, no. 4: 211–220. https://doi.org/10.1007/s40641-016-0050-x.

Maraun, D., F. Wetterhall, A. M. Ireson, et al. 2010. "Precipitation Downscaling Under Climate Change: Recent Developments to Bridge the Gap Between Dynamical Models and the End User." *Reviews of Geophysics* 48, no. 3. https://doi.org/10.1029/2009RG000314.

Maraun, D., M. Widmann, and J. M. Gutiérrez. 2019. "Statistical Downscaling Skill Under Present Climate Conditions: A Synthesis of the VALUE Perfect Predictor Experiment." *International Journal of Climatology* 39, no. 9: 3692–3703. https://doi.org/10.1002/joc.5877.

Maurer, E. P., H. G. Hidalgo, T. Das, M. D. Dettinger, and D. R. Cayan. 2010. "The Utility of Daily Large-Scale Climate Data in the Assessment of Climate Change Impacts on Daily Streamflow in California." *Hydrology and Earth System Sciences* 14, no. 6: 1125–1138. https://doi.org/10.5194/hess-14-1125-2010.

Meyer, J., I. Kohn, K. Stahl, K. Hakala, J. Seibert, and A. J. Cannon. 2019. "Effects of Univariate and Multivariate Bias Correction on Hydrological Impact Projections in Alpine Catchments." *Hydrology and Earth System Sciences* 23, no. 3: 1339–1354. https://doi.org/10.5194/hess-23-1339-2019.

Palazzi, E., L. Mortarini, S. Terzago, and J. von Hardenberg. 2019. "Elevation-Dependent Warming in Global Climate Model Simulations at High Spatial Resolution." *Climate Dynamics* 52, no. 5: 2685–2702. https://doi.org/10.1007/s00382-018-4287-z.

Pepin, N., M. Apple, J. Knowles, et al. 2025. "Elevation-Dependent Climate Change in Mountain Environments." *Nature Reviews Earth & Environment* 6, no. 12: 772–788. https://doi.org/10.1038/s43017-025-00740-4.

Pepin, N. C., E. Arnone, A. Gobiet, et al. 2022. "Climate Changes and Their Elevational Patterns in the Mountains of the World." *Reviews of Geophysics* 60, no. 1: e2020RG000730. https://doi.org/10.1029/2020RG000730.

Pichelli, E., E. Coppola, S. Sobolowski, et al. 2021. "The First Multi-Model Ensemble of Regional Climate Simulations at Kilometer-Scale Resolution Part 2: Historical and Future Simulations of Precipitation." *Climate Dynamics* 56, no. 11: 3581–3602. https://doi.org/10.1007/s00382-021-05657-4.

Reder, A., G. Fedele, I. Manco, and P. Mercogliano. 2025. "Estimating Pros and Cons of Statistical Downscaling Based on EQM Bias Adjustment as a Complementary Method to Dynamical Downscaling." *Scientific Reports* 15, no. 1: 621. https://doi.org/10.1038/s41598-024-84527-5.

Rolland, C. 2003. "Spatial and Seasonal Variations of Air Temperature Lapse Rates in Alpine Regions." *Journal of Climate* 16, no. 7: 1032–1046. https://doi.org/10.1175/1520-0442(2003)016<1032:SASVOA>2.0.CO;2.

Rota, F., G. Casazza, G. Genova, et al. 2022. "Topography of the Dolomites Modulates Range Dynamics of Narrow Endemic Plants Under Climate Change." *Scientific Reports* 12, no. 1: 1398. https://doi.org/10.1038/s41598-022-05440-3.

Switanek, M. B., P. A. Troch, C. L. Castro, et al. 2017. "Scaled Distribution Mapping: A Bias Correction Method That Preserves Raw Climate Model Projected Changes." *Hydrology and Earth System Sciences* 21, no. 6: 2649–2666. https://doi.org/10.5194/hess-21-2649-2017.

Tani, S., and A. Gobiet. 2019. "Quantile Mapping for Improving Precipitation Extremes From Regional Climate Models." *Journal of Agrometeorology* 21, no. 4: 434–443. https://doi.org/10.54386/jam.v21i4.278.

Tomasi, E., G. Franch, and M. Cristoforetti. 2025. "Can AI Be Enabled to Perform Dynamical Downscaling? A Latent Diffusion Model to Mimic Kilometer-Scale COSMO5.0_clm9 Simulations." *Geoscientific Model Development* 18, no. 6: 2051–2078. https://doi.org/10.5194/gmd-18-2051-2025.

Tootoonchi, F., J. O. Haerter, A. Todorović, O. Räty, T. Grabs, and C. Teutschbein. 2022. "Uni- and Multivariate Bias Adjustment Methods in Nordic Catchments: Complexity and Performance in a Changing Climate." *Science of the Total Environment* 853: 158615. https://doi.org/10.1016/j.scitotenv.2022.158615.

Vautard, R., N. Kadygrov, C. Iles, et al. 2021. "Evaluation of the Large EURO-CORDEX Regional Climate Model Ensemble." *Journal of Geophysical Research: Atmospheres* 126, no. 17: e2019JD032344. https://doi.org/10.1029/2019JD032344.

Verrall, B., and C. M. Pickering. 2020. "Alpine Vegetation in the Context of Climate Change: A Global Review of Past Research and Future Directions." *Science of the Total Environment* 748: 141344. https://doi.org/10.1016/j.scitotenv.2020.141344.

Volosciuk, C., D. Maraun, M. Vrac, and M. Widmann. 2017. "A Combined Statistical Bias Correction and Stochastic Downscaling Method for Precipitation." *Hydrology and Earth System Sciences* 21, no. 3: 1693–1719. https://doi.org/10.5194/hess-21-1693-2017.

Vrac, M., and P. Friederichs. 2015. "Multivariate—Intervariable, Spatial, and Temporal—Bias Correction." *Journal of Climate* 28, no. 1: 218–237. https://doi.org/10.1175/JCLI-D-14-00059.1.

Vrac, M., H. Loukos, T. Noël, and D. Defrance. 2025. "Should we Use Quantile-Mapping-Based Methods in a Climate Change Context? A "Perfect Model" Experiment." *Climate* 13, no. 7: 137. https://doi.org/10.3390/cli13070137.

Widmann, M., J. Bedia, J. M. Gutiérrez, et al. 2019. "Validation of Spatial Variability in Downscaling Results From the VALUE Perfect Predictor Experiment." *International Journal of Climatology* 39, no. 9: 3819–3845. https://doi.org/10.1002/joc.6024.

Wilks, D. S. 2011. *Statistical Methods in the Atmospheric Sciences*. Academic Press.

Wood, S. N. 2017. *Generalized Additive Models: An Introduction With R*. 2nd ed. Chapman and Hall/CRC.

Zscheischler, J., E. M. Fischer, and S. Lange. 2019. "The Effect of Univariate Bias Adjustment on Multivariate Hazard Estimates." *Earth System Dynamics* 10, no. 1: 31–43. https://doi.org/10.5194/esd-10-31-2019.

Zubler, E. M., S. C. Scherrer, M. Croci-Maspoli, M. A. Liniger, and C. Appenzeller. 2014. "Key Climate Indices in Switzerland; Expected Changes in a Future Climate." *Climatic Change* 123, no. 2: 255–271. https://doi.org/10.1007/s10584-013-1041-8.

Supporting Information

Additional supporting information can be found online in the Supporting Information section. **Figure S1:** Impact of random sampling for the two-fold splitting of the years on the evaluation metrics for spring (March–May) precipitation for domain-averaged metrics. **Figure S2:** Impact of random sampling for the two-fold splitting of the years on the evaluation metrics for spring (March–May) precipitation for grid-cell level metrics (RCM ensemble averages). **Figure S3:** Comparison of different lapse rates from observations and literature. Obs_Grid is the monthly mean of daily lapse rates based on the observational grid, while Obs_Station is the same but using the actual stations instead of the interpolated grid. The Clim suffix implies that monthly climatologies were calculated first and then the lapse rate based on the climatology. Literature based values: ListonElder20006 (?), which does not distinguish between minimum and maximum temperatures, Rolland2003 (?). **Figure S4:** Fraction of explained variance for each single PC. For temperature, the first PC, which has >90%, is not shown. See also Figures S6, S7 and S8 for the corresponding maps. **Figure S5:** Fraction of cumulative explained variance of the principle components (PC). See

10970088, 2026, 13, Downloaded from https://rmets.onlinelibrary.wiley.com/doi/10.1002/joc.70545 by CochraneItalia, Wiley Online Library on [03/11/2026]. See the Terms and Conditions (https://onlinelibrary.wiley.com/terms-and-conditions) on Wiley Online Library for rules of use; OA articles are governed by the applicable Creative Commons License

also Figures S6, S7 and S8 for the corresponding maps. **Figure S6:** Maps of the first nine principle components (PC) for precipitation. **Figure S7:** Maps of the first nine principle components (PC) for minimum temperature. **Figure S8:** Maps of the first nine principle components (PC) for maximum temperature. **Figure S9:** Metrics of the evaluation of the PCA-based downscaling in the perfect model setup (with upscaled observations) for precipitation. **Figure S10:** Metrics of the evaluation of the PCA-based downscaling in the perfect model setup (with upscaled observations) for minimum temperatures. **Figure S11:** Metrics of the evaluation of the PCA-based downscaling in the perfect model setup (with upscaled observations) for maximum temperatures. **Figure S12:** Maps of summer (JJA, June–July–August) median (p50) of daily maximum temperatures (tasmax). (a) Climatology and (b) differences to observations. Columns refer the different regional climate models. Rows are the raw model output, ba-mbcn is multivariate bias adjustment and ba-qdm is univariate bias adjustment. **Figure S13:** Domain-averaged bias for the different seasons and variables applying only bias adjustment and no downscaling. **Figure S14:** Domain-averaged summary evaluation metrics for minimum temperature downscaling. Boxplots summarise the 11 different RCMs. **Figure S15:** Domain-averaged summary evaluation metrics for maximum temperature downscaling. Boxplots summarise the 11 different RCMs. **Figure S16:** Domain-averaged summary evaluation metrics for precipitation downscaling. Boxplots summarise the 11 different RCMs. **Figure S17:** Maps of RCM ensemble averaged metrics for minimum and maximum temperatures. For bias the colour scale range has been capped to (−2, 2) and all values below/above are shown with the same colour as −2 and 2. Similarly, MAE has been capped to a maximum of 5. **Figure S18:** Maps of RCM ensemble averaged metrics for precipitation. **Figure S19:** Seasonal averages of Pearson correlation coefficients between the daily spatial fields of downscaled and observed maps. Boxplots summarise the 11 RCMs. **Figure S20:** Example maps for univariate and multivariate bias adjustment (BA) and downscaling (DS) for GERICS-REMO2015. (a) + (b) Maximum temperatures 2003-05-20. (c) + (d) Precipitation 2003-05-20. (a) + (c) Univariate BA (ba-qdm) and multivariate BA (ba-mbcn). (b) + (d) Downscaled maps. **Figure S21:** RCM ensemble averaged bias of minimum temperature for different seasonal metrics of mean and p(ercentiles). **Figure S22:** RCM ensemble averaged bias of maximum temperature for different seasonal metrics of mean and p(ercentiles). **Figure S23:** RCM ensemble averaged bias of precipitation for different seasonal metrics of mean and p(ercentiles). **Figure S24:** Precipitation 2003-11-01. (a) Observations at 1 km and upscaled to climate model scale (0.11°). (b) Raw climate model output (GERICS-REMO2015) and univariately bias adjusted. (c) Downscaled maps. **Figure S25:** Correlations between maximum temperature and precipitation in April for the different RCMs (rows) and univariate and multivariate BA and DS methods (columns). Correlations from the observations are in the bottom. **Figure S26:** RCM ensemble averaged bias of precipitation (pr), minimum temperature (tasmin) and maximum temperature (tasmax) for different seasonal metrics of mean and p(ercentiles). Shown are results from bias adjustment at the RCM scale without any downscaling.

10970088, 2026, 13, Downloaded from https://rmets.onlinelibrary.wiley.com/doi/10.1002/joc.70545 by CochraneItalia, Wiley Online Library on [03/11/2026]. See the Terms and Conditions (https://onlinelibrary.wiley.com/terms-and-conditions) on Wiley Online Library for rules of use; OA articles are governed by the applicable Creative Commons License